THEF-NIJM 93.03

Partial-wave analysis of all nucleon-nucleon scattering data below 350 MeV*

V.G.J. Stoks, R.A.M. Klomp, M.C.M. Rentmeester, and J.J. de Swart
Institute for Theoretical Physics, University of Nijmegen, Nijmegen, The Netherlands

Abstract

We present a multienergy partial-wave analysis of all NN scattering data below $T_{\rm lab} = 350$ MeV, published in a regular physics journal between 1955 and 1992. After careful examination, our final database consists of 1787 pp and 2514 np scattering data. Our fit to these data results in $\chi^2/N_{\rm df} = 1.08$, with $N_{\rm df} = 3945$ the total number of degrees of freedom. All phase shifts and mixing parameters can be determined accurately.

PACS numbers: 21.30.+y, 13.75.Cs, 11.80.Et, 12.40.Qq

*Published in Phys. Rev. C **48**, 792–815 (1993)

I. INTRODUCTION

In this paper we present the results of our partial-wave analyses of all NN scattering data below $T_{\rm lab} = 350$ MeV, where we mainly focus on the analysis of the np scattering data. The analysis of the pp data alone has already been published some time ago [1]. Preliminary results of a combined $pp + np$ analysis, including the pp as well as the np scattering data, have also been published [2, 3].

The abundance of accurate pp data below 350 MeV is such that a multienergy (m.e.) pp partial-wave analysis can be done successfully. Keeping the model input to a minimum, an excellent fit with $\chi^2/N_{\rm data} \approx 1$ is feasible. Here $N_{\rm data}$ denotes the number of scattering data. The m.e. phase shifts can be determined very accurately in such an energy-dependent analysis.

On the other hand, an analysis of only the np scattering data is much more difficult. The reason is that in case of pp scattering only the isovector partial waves contribute, whereas in case of np scattering also the isoscalar partial waves have to be taken into account. Moreover, the numerous np data are by far not as accurate as the pp data. In doing a partial-wave analysis of the np data it has therefore been customary to parametrize only the isoscalar lower partial waves, and to substitute for the isovector phase shifts the results from an analysis of the pp data. An exception is made for the $^1S_0$ phase shift which is usually also parametrized independently. The np isovector phase shifts can furthermore be modified to account for charge-independence breaking effects (e.g., Coulomb distortion and mass difference effects). The differences between the pp and np isovector phase shifts are then calculated via a theoretical model, where one assumes that one fully understands the breaking of charge independence and that one knows how to account for what one thinks to be the most important contributions to this breaking. Several different approaches have appeared in the literature, each leading to different results for the amount of charge-independence breaking. Therefore, an analysis of the np data is more model dependent than an analysis of only the pp data.

In the np analysis reported here we assume that charge independence is broken by the electromagnetic interaction, by the neutral-pion and charged-pion mass difference, and by the neutron and proton mass difference. The pion-nucleon coupling constants are taken to be charge independent. We refer to these charge-independence breaking corrections in the isovector partial waves as pion Coulomb corrections. For the $^1S_0$ partial waves we make an exception: the pp and np $^1S_0$ partial waves are parametrized independent of one another.

Our way of analyzing the pp scattering data has been explained in detail elsewhere [1, 4]. A similar procedure is applied to the analysis of the np data where the special treatment of the lower partial-wave np isovector phase shifts will be discussed in Sec. III B. In general our method fully exploits the fact that the long-range (electromagnetic and one-pion-exchange) part of the NN interaction is well known, whereas the short-range part of the interaction is sufficiently short ranged for the higher partial waves to be screened by the centrifugal barrier. This means that all partial waves with high angular momentum J are supposed to be well known, and only a relatively small number of lower partial waves need to be parametrized. The short-range part of the interaction in these lower partial waves is represented by an energy-dependent boundary condition (in our earlier papers referred to as the P matrix [5]), where the boundary-condition radius is chosen to be $b = 1.4$ fm. The boundary condition

is parametrized via a square-well potential of range $r = b$. The depth of this potential is independent of r, but is allowed to be energy dependent and different in each of the different partial waves. It can be shown that the depth of this potential is an analytic function of k^2, the c.m. three-momentum squared.

This analytic parametrization, together with the fact that we include the correct electromagnetic and one-pion-exchange potential tails, causes the energy dependence of the phase shifts in our m.e. partial-wave analysis to be described very well. As a consequence, we end up with an energy-dependent partial-wave solution which gives an excellent fit to all NN scattering data below $T_{\rm lab} = 350$ MeV. We find that for *all* lower partial waves the phase shifts are pretty well constrained by the NN scattering data as a whole. This means that our m.e. solution can also successfully be used to give fairly accurate predictions of NN scattering observables at any scattering angle and at any laboratory kinetic energy up to about 350 MeV.

Let us next compare our energy-dependent (or multienergy) analysis with an energy-independent (or single-energy) analysis. In such a single-energy (s.e.) analysis, the data in some particular energy interval are used to determine the phase shifts at one energy. This energy usually corresponds to the central value of that energy interval; however, this is not strictly necessary. Several of such energy-independent analyses at different energies provide at each of these energies a set of phase shifts with their errors. A shortcoming of energy-independent analyses is that the information about the overall energy dependence of the phase shifts cannot be incorporated. Also, the intermediate partial waves which are hard or impossible to determine (J equals 3 or 4, depending on the energy range) have to be fixed one way or another. We are in the fortunate position to be able to fix them at their values as provided by our energy-dependent m.e. solution, whereas in most s.e. analyses one has to resort to inaccurate potential-model predictions or to try to fit these phase shifts anyway. This means that the set of s.e. analyses covering, say, the 0–350 MeV region requires many more fit parameters than the m.e. analysis of the same energy region. Hence, the s.e. analyses are overparametrized and are much more sensitive to noise. This will be demonstrated in Sec. VI.

We want to stress that results from energy-independent analyses can only be properly judged by comparing them to the results of a corresponding energy-dependent analysis. The s.e. values for the phase shifts should scatter statistically around the curve representing the phase shifts as determined in the m.e. analysis. Of course, this is only true when the m.e. analysis one compares to is of good quality. We think that this is the case for the Nijmegen analyses, so we believe that for our analyses the "best" value for a particular phase shift is its value as obtained in the m.e. analysis, rather than the value as obtained in the s.e. analysis. However, since we do not include any constraints for energies larger than 350 MeV, our results for the phase shifts at the end of our energy range may be slightly off.

The outline of the paper is as follows. In Sec. II the model-independent long-range potential is given. Our method of parametrizing the lower partial-wave phase shifts using an energy-dependent boundary condition is briefly reviewed in Sec. III A. The treatment of the np isovector phase parameters is explained in Sec. III B. The construction of the total scattering amplitude including the various electromagnetic and one-pion-exchange contributions is briefly discussed in Sec. IV. Section V includes some details regarding our np database. The pp database was already discussed in our previous report [1]. The results of

the energy-dependent and energy-independent analyses are presented in Sec. VI.

II. THE POTENTIAL TAIL

In the Nijmegen partial-wave analyses we divide the NN interaction into two parts: a long-range part V_L which is well known and essentially model independent, and a short-range part V_S which is treated phenomenologically. The latter is represented by an energy-dependent boundary condition at $r = b = 1.4$ fm and will be discussed in the next section. Using the long-range potential V_L, the radial Schrödinger equation

$$(\Delta + k^2)\psi = 2M_r V\,\psi \tag{1}$$

is solved for $r > b$. Here Δ denotes the Laplacian and M_r is the reduced mass. Given the boundary condition and the solutions of the Schrödinger equation for each partial wave, it is easy to construct the partial-wave scattering amplitudes [4].

Relativistic effects are taken into account via the potential and by using the relativistic relation between the c.m. three-momentum squared k^2 and the laboratory kinetic energy $T_{\rm lab}$. For np scattering this relation is given by

$$k^2 = \frac{M_p^2 T_{\rm lab}(T_{\rm lab} + 2M_n)}{(M_p + M_n)^2 + 2T_{\rm lab}M_p}\ , \tag{2}$$

whereas for pp scattering it simply reads

$$k^2 = \tfrac{1}{2}M_p T_{\rm lab}\ . \tag{3}$$

For coupled channels Eq. (1) becomes a 2×2 matrix equation. The presence of the centrifugal barrier means that the Schrödinger equation needs only to be solved for a small number of lower partial waves ($J \le 4$). Still, the equation has to be solved for each energy at which experimental data have been measured.

The long-range potential V_L consists of an electromagnetic part $V_{\rm EM}$ and a nuclear part V_N. The electromagnetic interaction for pp scattering is the same as in our 0-350 MeV pp partial-wave analysis [1] and consists of the modified Coulomb potential V_C [6], the magnetic-moment interaction $V_{\rm MM}$ [7], and the vacuum polarization potential $V_{\rm VP}$ [8]. In the case of np scattering the electromagnetic interaction only consists of the magnetic-moment interaction. Explicitly, we can write the electromagnetic interaction as

$$\begin{aligned} V_{\rm EM}(pp) &= V_{C1} + V_{C2} + V_{\rm VP} + V_{\rm MM}(pp)\ , \\ V_{\rm EM}(np) &= V_{\rm MM}(np)\ , \end{aligned} \tag{4}$$

with

$$\begin{aligned} V_{C1} &= \frac{\alpha'}{r}\ , \\ V_{C2} &= -\frac{1}{2M_p^2}\left[(\Delta + k^2)\frac{\alpha}{r} + \frac{\alpha}{r}(\Delta + k^2)\right] \end{aligned}$$

$$\approx -\frac{\alpha\alpha'}{M_p r^2} \ ,$$

$$V_{\rm MM}(pp) = -\frac{\alpha}{4M_p^2 r^3}\left[\mu_p^2 S_{12} + (6+8\kappa_p)\mathbf{L}\cdot\mathbf{S}\right] \ , \tag{5}$$

$$V_{\rm MM}(np) = -\frac{\alpha\kappa_n}{2M_n r^3}\left[\frac{\mu_p}{2M_p}S_{12} + \frac{1}{M_r}(\mathbf{L}\cdot\mathbf{S}+\mathbf{L}\cdot\mathbf{A})\right] \ .$$

Here $\alpha' = 2k\eta/M_p$ with $\eta = \alpha/v_{\rm lab}$ the standard Coulomb parameter [9], $\mu_p = 2.793$ and $\mu_n = -1.913$ the proton and neutron magnetic moments, and $\kappa_p = \mu_p - 1$ and $\kappa_n = \mu_n$ their anomalous magnetic moments. Here we also introduced $\mathbf{A} = \frac{1}{2}(\boldsymbol{\sigma}_1 - \boldsymbol{\sigma}_2)$. The vacuum polarization potential [8] can be written as

$$V_{\rm VP} = \frac{2\alpha}{3\pi}\frac{\alpha'}{r}\int_1^\infty dx e^{-2m_e r x}\left(1+\frac{1}{2x^2}\right)\frac{\sqrt{x^2-1}}{x^2} \ , \tag{6}$$

where m_e is the electron mass. Obviously, the expressions above are only valid for $r > 0$.

The longest range of the nuclear interaction V_N is given by one-pion exchange (OPE). We make use of the fact that in NN scattering we encounter four different pseudovector coupling constants at the nucleon-nucleon-pion vertices: $f_{pp\pi^0}, f_{nn\pi^0}, f_{np\pi^-}$, and $f_{pn\pi^+}$. For the combinations that actually occur in the OPE potential, we use the following definitions:

$$\begin{aligned} \text{for } pp \to pp: &\ \ f_p^2 \equiv f_{pp\pi^0} f_{pp\pi^0} \ , \\ \text{for } np \to np: &\ \ f_0^2 \equiv -f_{nn\pi^0} f_{pp\pi^0} \ , \\ \text{for } np \to pn: &\ \ 2f_c^2 \equiv f_{np\pi^-} f_{pn\pi^+} \ . \end{aligned}$$

In case of charge symmetry, one has $f_p^2 = f_0^2$, whereas in case of charge independence, one has $f_p^2 = f_0^2 = f_c^2$. For pp scattering the OPE potential can be written as

$$V_{\rm OPE}(pp) = f_p^2 V(m_{\pi^0}) \ , \tag{7}$$

and for np scattering it reads

$$V_{\rm OPE}(np) = -f_0^2 V(m_{\pi^0}) + (-)^{I+1} 2 f_c^2 V(m_{\pi^+}) \ , \tag{8}$$

where I denotes the total isospin, and where we introduced $V(m)$, which for large values of r is given by

$$V(m) = \frac{1}{3}\left(\frac{m}{m_s}\right)^2 \frac{e^{-mr}}{r}\left[(\boldsymbol{\sigma}_1\cdot\boldsymbol{\sigma}_2) + S_{12}\left(1+\frac{3}{(mr)}+\frac{3}{(mr)^2}\right)\right] \ . \tag{9}$$

A scaling mass m_s is introduced in order to make the pseudovector coupling constant f dimensionless. It is conventionally chosen to be the charged-pion mass. When we solve the Schrödinger equation for $r > b$ the potential tail of Eq. (9) is multiplied with an energy-dependent factor M/E, where M is the nucleon mass and E is the c.m. energy. Leaving out this M/E factor in the potential tail results in a small rise in $\chi^2_{\rm min}$. In view of the well-known expression for the OPE scattering amplitude in Born approximation (which is simply related to the OPE potential), we believe it is better to include this M/E factor.

The nuclear interaction also contains contributions of intermediate range due to the exchange of heavier mesons (like ρ, ω, η). For these heavier-boson-exchange (HBE) contributions we use the HBE contributions from the Nijmegen potential [10] denoted by $V^N_{\rm HBE}$. For $r \gtrsim 1.5$ fm, the various realistic potential models that have appeared in the literature are very much alike. This allows us to make a choice for the boundary-condition radius b such that the tail of the nuclear potential used for $r > b$ does not introduce too much model dependence. We choose $b = 1.4$ fm.

Although the inclusion of the HBE contributions gives an improved fit over the analysis where we only include the OPE potential, there are still indications that this nuclear potential tail is not perfect. As discussed in our report on the *pp* analysis [1], an improvement can be obtained by multiplying the HBE contributions for the singlet partial waves with a factor $f^s_{\rm med}$. In the present analysis we extend this procedure to the *np* partial waves as well, i.e., for all singlet partial waves up to $J = 4$ the HBE contributions are multiplied with $f^s_{\rm med} = 1.8$. So the nuclear part of the potential tail is given by $V_N = V_{\rm OPE} + V^N_{\rm HBE}(f^s_{\rm med})$.

III. PARAMETRIZATION OF THE LOWER PARTIAL WAVES

A. Boundary-condition parametrization

The phenomenology necessary to describe the short-range interaction enters our method via a boundary condition at $r = b = 1.4$ fm,

$$P_\beta(b;k^2) = b\left[\frac{d\chi_\beta(r)}{dr}\chi^{-1}_\beta(r)\right]_{r=b} , \tag{10}$$

where β denotes the quantum numbers (l, s, J) of the particular partial wave to be parametrized. The radial wave function $\chi(r)$ which enters this expression can also be represented by the solution of the Schrödinger equation for $r < b$ in the presence of the short-range potential V_S. In the trivial case that $V_S(r) = 0$ for $r < b$, this equation can be solved exactly and the radial wave function is a spherical Bessel function, $\chi_l(r) = krj_l(kr)$. The resulting logarithmic derivative $P_{{\rm free},l}(b;k^2)$ we refer to as the free boundary condition. When $V_S(r)$ is a constant, independent of r, its contribution can be absorbed into the parameter k^2 and we have

$$P_\beta(b;k^2) = P_{{\rm free},l}(b;k^2 - 2M_r V_{S,\beta}) \ . \tag{11}$$

Obviously, this substitution still remains valid when V_S is an analytic function of the energy, and in our analyses the short-range interaction is parametrized by such an energy-dependent, but r-independent square-well potential of range $r = b$. Its depth $V_S(k^2)$ is allowed to be different for each different partial wave. It is parametrized as

$$V_{S,\beta}(k^2) = \frac{1}{2M_r}\sum_{n=0}^{N} a_{n,\beta}(k^2)^n \ . \tag{12}$$

When all $a_{n,\beta}$ are equal to zero, $P_\beta = P_{{\rm free},l}$.

In the case of two coupled channels, we start with two single-channel parametrizations P_a for $l = J-1$ and P_b for $l = J+1$, which form the diagonal elements of a 2×2 matrix. The off-diagonal elements are then parametrized as a power series in k^2. A convenient parametrization is given by

$$P = \begin{pmatrix} \cos\theta & \sin\theta \\ -\sin\theta & \cos\theta \end{pmatrix} \begin{pmatrix} P_a & 0 \\ 0 & P_b \end{pmatrix} \begin{pmatrix} \cos\theta & -\sin\theta \\ \sin\theta & \cos\theta \end{pmatrix} , \tag{13}$$

where the angle θ is some smooth function of k^2.

Due to the fact that for $r > b$ we include the correct long-range potential V_L (see Sec. II), the parametrization of the short-range potential $V_{S,\beta}$ only requires very few parameters. Even for the lowest partial waves with $0 \leq J \leq 2$, only one parameter (i.e., an energy-independent short-range potential) already gives a very reasonable description of the corresponding phase shifts. This is demonstrated in Fig. 1. Here the solid curve represents the pp $^3P_0$ phase shift as a function of the energy, as obtained in our m.e. analysis (see Sec. VI). The dashed line represents this phase shift using $V_S = 0$, i.e., $P(^3P_0) = P_{\rm free,1}$. The disagreement with the m.e. result is rather large, although the general characteristics are already there. Introducing only one parameter, i.e., an energy-independent short-range potential, the resulting phase shift (represented by the dotted curve) is already very close to the m.e. result. Similar results are obtained for the other lower partial waves. In general, the introduction of a second or third parameter in the parametrization of the short-range potential in the lowest partial waves is in a sense only necessary to fine-tune the corresponding phase shift.

B. Treatment isovector np phase parameters

Contrary to the analysis of the pp scattering data, in the analysis of the np scattering data isoscalar partial waves also contribute. This means that one has to determine almost twice as many partial waves. A problem arises due to the fact that the np scattering data are by far not as accurate as the pp scattering data; so they cannot accurately pin down all these lower partial waves simultaneously. In doing a partial-wave analysis of np scattering data it has therefore been customary to parametrize the isoscalar lower partial waves, and to substitute for the isovector phase shifts the results from an analysis of the pp scattering data, whether or not adjusted for Coulomb distortion and mass difference effects. Several ways for making such pp-to-np corrections have appeared in the literature.

For example, in the Virginia Polytechnic Institute and State University (VPI-SU) partial-wave analyses by Arndt and co-workers [11, 12, 13], the np shifts are represented by series expansions which are based on a plane-wave Born approximation calculation to a combination of a t-channel (m_{π^0}) and a u-channel ($m_{\pi^\pm}$) pole. The corresponding pp phase shifts are then obtained from this parametrization by only including the t-channel pole, and multiplying the result with a Coulomb penetration factor. A problem with this representation of the charge-independence breaking in the VPI-SU analyses is that in these analyses the pion-mass difference not only appears in the OPE contribution to the phase shifts, but also in the phenomenological parametrization of the short-range interaction. This introduces an additional

charge-independence breaking. A more serious shortcoming is that the Coulomb penetration factor overestimates the effect of the Coulomb distortion. The pp phase shifts should be calculated in Coulomb distorted-wave Born approximation, rather than in plane-wave Born approximation multiplied by the Coulomb penetration factor. The latter calculation requires a substantially higher pion-nucleon coupling constant if one wants to arrive at the same numerical value for the pp phase shift as obtained with the proper Coulomb distorted-wave calculation using a low coupling constant [14, 15]. This explains the fact that in the VPI-SU analysis of only the pp data, the "best" fit is obtained with $f_p^2 \approx 0.080$. However, the most recent VPI-SU analyses include the Coulomb distorted-wave calculation for the pp phase shifts using the low value $f^2 = 0.075$ for both the neutral and charged pion-nucleon coupling constants with good results [16].

Another way for taking into account the Coulomb effects is the Graz prescription [17, 18, 19], which is used in the TRIUMF analyses by Bugg and co-workers [20, 21, 22, 23]. In the Graz prescription the pp phase shift is written as the sum of a purely nuclear phase shift δ^N and a residual phase shift δ^R which represents the contribution due to the Coulomb interaction. It is then possible [17] to derive an expression for δ^R in terms of δ^N, which can serve in two ways. Either isovector np phase shifts are known and the corresponding pp phase shifts can be calculated, or pp phase shifts are available which can then be used to solve for the corresponding isovector np phase shifts in an iterative way. Either way can be used in a partial-wave analysis. A serious shortcoming of the Graz method is that one only corrects for the Coulomb interaction, whereas the neutral-to-charged pion mass difference is not accounted for. As will be demonstrated below, the effects on the phase shifts due to the pion-mass difference are equally important as the effects due to the Coulomb interaction, so they should not be neglected.

In the Nijmegen analyses we include the effects due to the Coulomb interaction, but we also explicitly account for the neutral-to-charged pion mass difference. First we calculate pp phase shifts by solving the Schrödinger equation for some realistic nuclear potential V_N in the presence of the Coulomb potential $V_{C1} = \alpha'/r$. In order to obtain the corresponding np phase shifts, the pp OPE part of the nuclear potential is replaced by the np OPE potential. So the corresponding potentials for these two cases are given by

$$\begin{aligned} pp &: V = V_N + V_{C1} \ , \\ np &: V = [V_N - V_{\rm OPE}(pp)] + V_{\rm OPE}(np) \ , \end{aligned} \tag{14}$$

where the OPE potentials, properly modified by a form factor to account for the spatial extension of the nucleons and pions, are given in Eqs. (7) and (8). In our calculations we use an exponential form factor [10] $F(\mathbf{k}^2) = \exp[-(\mathbf{k}^2 + m_\pi^2)/\Lambda^2]$ with $\mathbf{k}^2$ the momentum transfer squared and Λ a cutoff mass. At the pion pole $F(\mathbf{k}^2 = -m_\pi^2) = 1$.

Substituting these OPE potentials into Eq. (14) the pp-np phase-shift differences can in principle be calculated for several values of the pion-nucleon coupling constants. In that way we can also allow for a possible breaking of charge independence in the coupling constants and the pion Coulomb corrections are essentially parametrized via these coupling constants. The dependence of our analyses on the pion-nucleon coupling constants is investigated elsewhere [2, 24]. In this paper we assume a common charge-independent value $f^2 = 0.075$ for all pion-nucleon coupling constants, which is consistent with the result of [24].

For the nuclear potential V_N we use an updated version of the Nijmegen soft-core potential [10]. The parameters of this Nijm92*pp* potential [25] have been fitted to the *pp* scattering data below 350 MeV with a χ^2 per datum of 1.4. The dependence on the particular nuclear potential model that is used is rather small. For instance, when we use the original Nijmegen potential [10] for V_N, the m.e. *np* analysis with the corresponding pion Coulomb corrections results in a χ^2 which is 7.4 higher than the analysis where we use the pion Coulomb corrections calculated via the Nijm92*pp* potential. Similarly, for the parametrized Paris potential [26] the difference in χ^2 is only 2.5.

In Table I we demonstrate the effect on some of the phase shifts when we include the difference between the OPE potentials for *pp* and *np* scattering. We first give the *pp* phase shifts of the Nijm92*pp* potential including the Coulomb interaction, then the phase shifts after the Coulomb interaction is removed, while in the last column we list the *np* phase shifts as obtained after also correcting for the pion-mass difference. The significance of the inclusion of this modification in the OPE potential is also apparent from the analysis of the *np* scattering data. When we only correct for the absence of the Coulomb interaction in the *np* isovector partial waves (which essentially corresponds to applying the Graz prescription), the m.e. analysis of the *np* data gives a χ^2 which is 22 higher than the analysis where we also include the modification in the OPE potential due to the pion-mass difference in these partial waves.

The *np* $^1S_0$ partial wave is parametrized independently of the *pp* data (as is also customary in other analyses). The reason is that there is clear evidence for breaking of charge independence in the $^1S_0$ scattering lengths which carries over into an approximately 2° phase-shift difference of the $^1S_0$ phase shifts for the *pp* and *np* systems at higher energies (see Sec. VI). These differences cannot be explained as being only due to the difference between the *pp* and *np* OPE potentials.

Before concluding this section we summarize the way the lower partial waves are parametrized in our analyses. The *pp* lower partial waves up to $J = 4$ are parametrized via an energy-dependent, but r-independent square-well potential. The same type of parametrization is used for the *np* isoscalar partial waves up to $J = 4$ and for the *np* $^1S_0$ partial wave. The *np* isovector phase shifts (except the $^1S_0$ phase shift) are obtained from the corresponding *pp* phase shifts by including the pion Coulomb corrections described above. (A possible difference between the neutral-pion and charged-pion coupling constants can also be accounted for and has been discussed elsewhere [2, 24].) For the intermediate partial waves ($5 \leq J \leq 8$) we use the phase shifts calculated via the OPE plus HBE contributions of the Nijmegen potential [10]. All higher partial waves are given by the OPE phase shifts, adjusted for electromagnetic effects (Coulomb, magnetic moment, vacuum polarization) where necessary.

IV. THE SCATTERING AMPLITUDE

In this section we briefly summarize the expressions for the various parts of the scattering amplitude for reasons of completeness. The wave function for the *NN* scattering process can asymptotically be written as

$$\psi^s_m(\mathbf{r}) \sim e^{ikz}\xi^s_m + \frac{e^{ikr}}{r}\sum_{s',m'}\xi^{s'}_{m'}M^{s's}_{m'm}(\theta,\phi)\ , \tag{15}$$

where ξ^s_m denotes the spin state, and $M^{s's}_{m'm}(\theta,\phi)$ are the matrix elements of the spin-$\frac{1}{2}$ spin-$\frac{1}{2}$ scattering amplitude with θ and ϕ the polar angles. All NN scattering observables can be expressed in terms of the M-matrix elements [27, 28]. The partial-wave decomposition is given by

$$M^{s's}_{m'm}(\theta,\phi) = \sum_{l,J,l'}\sqrt{4\pi(2l+1)}\,Y^{l'}_{m-m'}(\theta,\phi)C^{l'\ s'\ J}_{m-m'\ m'\ m}\,i^{l-l'}\frac{\langle l',s'|S^J-1|l,s\rangle}{2ik}C^{l\ s\ J}_{0\ m\ m}\ , \tag{16}$$

where $C^{l\ s\ J}_{m_l\ m_s\ M}$ is a Clebsch-Gordan coefficient and $Y^l_m(\theta,\phi)$ is a spherical harmonic.

Using the familiar nuclear-bar phase shifts and mixing parameters, the spin-triplet coupled S matrix with total angular momentum J is parametrized as

$$S^J = \begin{pmatrix} e^{2i\delta_1}\cos 2\varepsilon_J & ie^{i(\delta_1+\delta_2)}\sin 2\varepsilon_J \\ ie^{i(\delta_1+\delta_2)}\sin 2\varepsilon_J & e^{2i\delta_2}\cos 2\varepsilon_J \end{pmatrix}\ . \tag{17}$$

with $\delta_1 = \delta_{J-1,J}$ and $\delta_2 = \delta_{J+1,J}$. For the spin-singlet spin-triplet S matrix with $l = J$ we have

$$S^J = \begin{pmatrix} e^{2i\delta_l}\cos 2\gamma_l & ie^{i(\delta_l+\delta_{l,l})}\sin 2\gamma_l \\ ie^{i(\delta_l+\delta_{l,l})}\sin 2\gamma_l & e^{2i\delta_{l,l}}\cos 2\gamma_l \end{pmatrix}\ , \tag{18}$$

where γ_l is the nuclear-bar spin-flip mixing angle as introduced by Gersten [29]. For identical particle scattering (i.e., for pp scattering) it is identically zero, and the S matrix for $l = J$ decouples. In our analyses we do not (yet) parametrize the spin-flip mixing angles. We only include the contributions due to the neutron-proton mass difference in the np magnetic-moment and OPE scattering amplitudes. This implies, for example, that we explicitly distinguish between scattered and recoil analyzing power data in np scattering.

The phase shifts which parametrize the partial-wave S matrix can conveniently be written as a sum of two parts: the purely electromagnetic phase shifts, and the phase shifts of the nuclear plus electromagnetic interaction with respect to electromagnetic wave functions. Because of the short range of the nuclear interaction the latter phase shifts rapidly approach their OPE values for increasing orbital angular momentum J, so only a limited number need to be parametrized explicitly. Moreover, the electromagnetic part of the scattering amplitude is known explicitly.

The total scattering amplitude $M_{\rm tot}$ can now symbolically be written as

$$M_{\rm tot} = M_{\rm EM} + M_{\rm OPE} + \sum_{l=0}^{l_{\rm max}}(M_{{\rm par},l} - M_{{\rm OPE},l})\ , \tag{19}$$

where $l_{\rm max}$ denotes the highest orbital angular momentum of the partial wave that is explicitly parametrized (in our analysis by means of a boundary condition or via the phase shifts of the OPE plus HBE contributions of the Nijmegen potential). The expressions for the partial-wave OPE amplitudes in plane-wave Born approximation can easily be derived.

For np the mass differences between neutron and proton and between neutral and charged pions can explicitly be accounted for (see, e.g., Refs. [15, 28]). The pp OPE amplitude has to be calculated in Coulomb distorted-wave Born approximation to account for the Coulomb distortion effects. The evaluation has to be done numerically, because it involves the evaluation of integrals of Coulomb functions with Yukawa potentials. The expressions for the M-matrix elements can be found in Ref. [15].

The various parts of the electromagnetic amplitude $M_{\rm EM}$ correspond to the various parts of the electromagnetic potentials as given in Eq. (4). In evaluating these parts one has to correct for the fact that each contribution is included separately. The details of these modifications are extensively discussed in Ref. [7] and will not be repeated here. Here we merely list the various amplitudes.

For pp scattering we have

$$M_{\rm EM}(pp) = M_{C1} + M_{C2} + M_{\rm MM} + M_{\rm VP} \ . \tag{20}$$

The point-charge Coulomb potential V_{C1} gives rise to the well-known scattering amplitude

$$\begin{aligned} f_{C1}(\theta) &= \frac{1}{2ik}\sum_l (2l+1)\left[e^{2i(\sigma_l-\sigma_0)}-1\right]P_l(\theta) \\ &= -\frac{\eta}{k}\,\frac{e^{-i\eta\ln\frac{1}{2}(1-\cos\theta)}}{1-\cos\theta} \ , \end{aligned} \tag{21}$$

with $P_l(\theta)$ the Legendre polynomials, and the Coulomb phase shifts defined as $\sigma_l = \arg\Gamma(l+1+i\eta)$. The properly antisymmetrized M-matrix elements are now given by

$$\langle s', m'|M_{C1}(\theta)|s, m\rangle = [f_{C1}(\theta) + (-)^s f_{C1}(\pi-\theta)]\delta_{s's}\delta_{m'm} \ .$$

For the relativistic correction V_{C2} to the Coulomb potential we use the $1/r^2$ approximation of Eq. (5). The advantage of using this approximation is that it can be absorbed into the centrifugal barrier, and the radial Schrödinger equation with $V_{C1}+V_{C2}$ can be solved exactly in terms of Coulomb functions with non-integer l. The phase shifts of V_{C2} are then given by

$$\rho_l = \sigma_\lambda - \sigma_l + \frac{(l-\lambda)\pi}{2} \ , \tag{22}$$

where λ satisfies $\lambda(\lambda+1) = l(l+1) - \alpha\alpha'$. The corresponding amplitude reads

$$f_{C2}(\theta) = \frac{1}{2ik}\sum_l (2l+1)e^{2i(\sigma_l-\sigma_0)}\left[e^{2i\rho_l}-1\right]P_l(\theta) \ , \tag{23}$$

and again the corresponding M-matrix elements are obtained via antisymmetrization.

Expressions for the vacuum polarization amplitude and for the vacuum polarization phase shifts τ_l were derived by Durand [8]. In our calculations we use modifications to these expressions [30] to be able to extend the energy range to energies below $T_{\rm lab} \lesssim 1$ MeV. For the expressions for the magnetic-moment amplitudes in both pp and np scattering we again refer to Ref. [7].

V. THE DATA

Our data set consists of all *pp* and *np* data below $T_{\rm lab} = 350$ MeV published in a regular physics journal between January 1955 and December 1992. We therefore do not include preliminary data that have only appeared in conference proceedings. We regard it more appropriate to wait with the inclusion of these data into our database until the experimentalists have published their final results in a regular physics journal. In most cases, however, we do have their preliminary data and we have investigated how they fit in with the other data in our database. Examples of such data are *pp* differential cross sections $\sigma(\theta)$, analyzing powers A_y, and depolarizations D (all at 12.0 MeV), and analyzing powers A_y at 25.68 MeV by the Erlangen group [31, 32]. For *np* we mention the spin correlation coefficients A_{yy} between 18 and 50 MeV by the Karlsruhe group [33]. We find that these data have no major consequences for the conclusions drawn in this paper using the present database.

Most of the data can be found in the nucleon-nucleon scattering data tables of Bystricky and Lehar [34, 35]. We have consulted all original papers while building our database. This implies that we have corrected for some minor printing errors in the Scattering data tables. We have also included data that are not contained in these tables. These groups are denoted by a dagger in Table II. Our database was composed in close collaboration with the VPI-SU group. Data that are not included in the data set NN931 of the VPI-SU partial-wave analysis SAID [36] (mainly because they do not live up to our rejection criteria anyway) are denoted by an asterisk.

Dispersion relation predictions [37] and data obtained through quasielastic scattering are not included as experimental data. We also exclude *pp* total cross-section data ($\sigma_{\rm tot}$, $\Delta\sigma_{\rm L}$, $\Delta\sigma_{\rm T}$), because of ambiguities in their definition and because it is not always clear how the Coulomb-nuclear interference term has been treated by the experimentalists.

A. pp data

The *pp* scattering data can be found in Table I of a previous report [1]. In the meantime we have added three groups of polarization data [38, 39, 40], which were published after we finished our *pp* analysis. The very accurate 10 *pp* polarization data by the Zürich group [38] at 50.04 MeV were analyzed and discussed in detail in Ref. [41]. There it is shown that the magnetic-moment interaction has to be included in order to describe these data properly. A recent absolute calibration measurement of the transverse analyzing power in proton-carbon elastic scattering [42] implied that these 50.04 MeV A_y data should be renormalized by a factor 1.0069, where the previous overall scale uncertainty of 2% should be reduced to 0.39%. We use the renormalized data.

The other new experiments comprise 1 A_y datum at 183.1 MeV [39] and 20 A_y data at 185.4 MeV [40]. The corresponding χ^2 values for these three groups in the *pp* analysis are as follows:

$T_{\rm lab}$(MeV)	χ^2	$N_{\rm data}$	Reference
50.04	4.98	10	[38, 42]
183.1	2.28	1	[39]
185.4	12.96	20	[40]

Including these data, our *pp* database now comprises 215 groups with a total of 1656 scattering observables or, counting the 131 normalization data, 1787 scattering data. Of these groups, 22 have a floated normalization, which means that we keep their normalization free.

We have taken the opportunity to reinvestigate the parametrization of the lower partial waves. The reason is that the seven-parameter energy dependence of the $^1S_0$ phase shift in our original *pp* analysis [1] showed noise. Also, we had to include $\delta(^1S_0) = 19^\circ \pm 2^\circ$ at 425 MeV as an extra datum to ensure a proper energy dependence at the end of our energy range, near 350 MeV. This should be compared with the *np* analysis where we find that the boundary condition for the $^1S_0$ phase shift can be parametrized with three parameters and where we do not have to include an extra datum at 425 MeV. We have reparametrized the boundary condition for the *pp* $^1S_0$ phase shift where we now need four parameters and where we can drop the constraint at 425 MeV. Although the $\chi^2_{\rm min}$ with this parametrization is about 12 higher than the $\chi^2_{\rm min}$ with the former parametrization, the smoothness of the energy dependence of the m.e. phase shifts strengthens our belief that the new parametrization is to be preferred over the old one. Moreover, when we start with four parameters for the $^1S_0$ and successively add one parameter at a time, the χ^2 only showed a significant drop after we added the seventh parameter. This is an indication that with seven parameters the $^1S_0$ was overparametrized. In our present energy-dependent *pp* analysis we need 21 parameters to parametrize the lower partial-wave boundary conditions, which makes the number of degrees of freedom $N_{\rm df} = 1613$.

B. np data

All *np* data are listed in Table II. We give them explicitly, because with the *pp* database as given in Table I of Ref. [1] we have provided a self-contained and complete database. In Table II all analyzing powers (scattered or recoil) and polarizations (beam or target) are denoted by the same symbol P, although in our actual calculations an explicit distinction has been made whenever this was applicable.

Starting with the complete *np* database of 3298 scattering observables, the boundary-condition parameters were adjusted to obtain $\chi^2_{\rm min}$. As a criterion for the total number of boundary-condition parameters to be fitted we apply the rule that we only include an additional parameter if this really improves the quality of the fit. All data which were more than three standard deviations off were rejected and the parameters were adjusted again. Some groups have an experimental normalization error that contributes more than nine to χ^2, probably due to an underestimation of systematic errors by the experimentalists. These groups are floated by us and in Table II we have put their original experimental normalization error between parentheses in the column labeled "% error". Groups that have an improbably low or high χ^2 are also rejected. These groups are indicated by "f" and "m" in the column

labeled "Comment," respectively. We explicitly checked that for our final solution these adjustments to our database are still justified.

Making all these adjustments results in the rejection of 932 data, which gives us our final data set of 211 groups with a total of 2366 *np* scattering observables. The number of groups with an experimental normalization error is 148, so we have 2514 scattering data. The number of groups that are floated is 16. To parametrize the lower partial waves we need 18 boundary-condition parameters. The total number of degrees of freedom is $N_{\rm df} = 2332$.

Our total database including the *pp* as well as the *np* data now comprises 4301 scattering data and the number of degrees of freedom is 3945. We need 39 parameters for the boundary conditions of the lower partial waves. The multiplication parameter for the HBE contributions of the singlet waves, $f^s_{\rm med} = 1.8$, and the boundary-condition radius $b = 1.4$ fm were *not* fitted but fixed at these values. They are therefore not included in $N_{\rm df}$.

A large number of *np* total cross-section data are not explicitly included in our database. These total cross-section data were measured to search for a possible fluctuation in the energy dependence of the *np* total cross section. The reason was that in their measurement of the cross section at low energies, Hrehuss and Czibók [52] found a small but statistically significant periodical fluctuation in the energy dependence of the cross section. Shortly after their publication, total cross-section measurements were reported by several other groups [49, 153, 154, 155], who did not find such a structure. We do not find any evidence for a periodical fluctuation in the cross section either. From Fig. 3 of Ref. [52], the oscillatory behavior is seen to be largest at $\theta_{\rm c.m.} = 170^\circ$. And it is just these $\sigma(170^\circ)$ data that do not fit in with our analysis. Three of the groups of total cross-section measurements contain very many data: 1652 data in Ref. [153], 800 data in Ref. [154], and 425 data in Ref. [155]. This number of 2877 total cross-section data in the 0–30 MeV energy range should be compared with our set of 2514 much more diverse data (cross sections, analyzing powers, spin correlations, rotation parameters, etc.) in the 0–350 MeV energy range. To analyze these 2514 scattering data we have to solve the Schrödinger equation for the lowest partial waves at approximately 375 different energies. When we also want to include the 2877 total cross-section measurements we have to solve the Schrödinger equation for an additional ∼2850 energies. In our point of view, the very small amount of new information these data possibly contain does not justify the enormous increase in computer storage and time, which would be needed if we were to include them in our final database. Since there are only 17 data in the Harwell measurement by Clements and Langsford [49], we decided to keep this small group in our database, and to study the other three groups separately.

First, we compared the total cross sections as predicted by our analysis with the experimental values given by these three groups. For the 1652 Washington data [153] the prediction is excellent and we find $\chi^2 = 1411.9$. For the 425 LINAC data [155] we find that there are nine data points which are more than three standard deviations off. Leaving out these nine data points we find the reasonable value of $\chi^2 = 558.3$ for the remaining 416 data. At the low end of the energy range the Karlsruhe data [154] are too low when compared with the prediction of our m.e. analysis, whereas at the high end of the energy range they are too high. A similar observation is made by these authors themselves [154] when they compare their results with other measurements. Our χ^2 prediction for these data is $\chi^2 = 4474$, which is much too high for 800 data. This group of data will therefore no longer be included in any of our analyses.

In our next step the data in the remaining two groups were clustered at a number of central energies and then included in the database of the analysis. For the data of the LINAC group each successive set of three energies was in that way represented by one (properly weighted) datum at the central energy. This resulted in a group of 142 data. A similar procedure was used for the Washington data, where now each successive group of seven data was lumped into a datum at one energy, resulting in a group of 236 data. Including these two groups in our database, one of the adjusted LINAC data and two of the adjusted Washington data are found to be more than three standard deviations off. Performing the m.e. *np* analysis after removing these three data, we find $\chi^2 = 147.6$ for the 141 adjusted LINAC data and $\chi^2 = 233.9$ for the 234 adjusted Washington data. The χ^2 on the other 2514 data of our database rises with 8.3. However, we still decided not to include these data in our database. As already stated above, their inclusion requires an enormous increase in computer storage and time, whereas their influence is relatively small. The only conclusion we want to make here is that the LINAC and Washington data are in agreement with the other data in our database and with the predictions of our partial-wave solution. The Karlsruhe total cross-section data, on the other hand, are very much off.

Next we discuss some of the groups of data we found had to be rejected. All 282 Harwell differential cross-section data by Scanlon *et al.* [85] at 14 energies between 22.5 and 108.5 MeV are rejected by us. The reason is that most of these groups have a large χ^2 and the phase shifts determined in a single-group analysis differ very much from their m.e. values. From this we conclude that there is something systematically wrong with these data. We therefore decided to reject the entire experiment, including the groups at 22.5 and 27.5 MeV which appear not to be in conflict with the other data. Our rejection of these data is in agreement with earlier analyses by other groups who also find them to be erroneous (see, e.g., [156]). On the other hand, the Harwell total cross-section data [69] can be described very well in our analysis. Of the 17 Harwell polarization data at 77.0 MeV [113], three data are more than three standard deviations off. After removing these data the remaining group of 14 data still has a χ^2 which is improbably high.

The group of 32 differential cross-section data at 96.0 MeV by the Uppsala group [119] has a large χ^2 which is mainly due to the backward-angle data. These backward-angle data are much higher than the prediction of our m.e. analysis. The Uppsala data were obtained by taking the weighted mean of five measurements in different (but overlapping) angle regions. We have tried to include these original measurements [157] in our m.e. analysis, but we found that only the group which does not contain any backward-angle data is in good agreement with the other data in our database. Also, single-group analyses of these data result in phase shifts which are very much in disagreement with our m.e. results. For example, in some of these single-group analyses the resulting ε_1 mixing parameter is larger than 10°. In view of our m.e. result for ε_1, we believe that such a solution is totally unacceptable. The Uppsala group [119] states that the slope of their backward-angle data indicates a larger importance of $L \geq 3$ phase shifts than previously assumed. However, in our experience 96.0 MeV is too low an energy for $L \geq 3$ phase shifts to be accurately determined in a single-group or s.e. analysis. On the other hand, these phase shifts are already fixed pretty well in the m.e. partial-wave analysis (i.e., by the data at higher energies), so there is not too much room for varying these phase shifts. We therefore believe that these data are in error and hence we do not include them in our final database.

The group of 13 Harvard cross-section data at 152.0 MeV [132] does not contain a normalization error. As such it gives a very high χ^2. Floating this group reveals that the slope is in error, and the resulting χ^2 is still much too high.

One of the groups of Los Alamos cross-section measurements by Bonner *et al.* [133] (at 194.5 MeV) has a χ^2 which is somewhat higher than allowed according to our three standard deviation criterion, so it is removed from our database. The same applies to the 21 cross-section data at 200.0 MeV by Kazarinov and Simonov [138]. These latter data were also rejected in the partial-wave analysis by Dubois *et al.* [21].

All nine groups of Princeton differential cross-section data by Shepard *et al.* [136] had to be floated by us, because their normalization errors gave an improbably high contribution to χ^2. Even then each group has a χ^2 which is improbably high. Therefore, all 158 data are rejected by us. Also the four Princeton total cross-section data [145] give a χ^2 which is much too high.

Finally, we also reject the eight groups of SIN cross-section data by Hürster *et al.* [139], which were measured in steps of 20 MeV starting at 200 MeV. The reason is the following. For each group the first few data with c.m. angles of about 140°–150° are more than three standard deviations off. When we remove these data and refit our model parameters, again the next one or two angles are more than three standard deviations off, so we have to reject these as well. Refitting again yields other angles which have to be rejected. We therefore believe there is something systematically wrong with the shape of these cross-section measurements. It is in disagreement with the shape resulting from the other data in this energy region, so all 276 data are rejected by us.

This explains the bulk of data rejected by us. The remaining 87 *np* data are rejected because of similar reasons: Some groups have a χ^2 which is improbably low, some individual data are more than three standard deviations off, etc. The number of 932 *np* data that we reject appears to be large. One can argue that it could be possible that these rejected data contain important physics, which our present approach cannot handle. However, we explicitly checked that the m.e. values for the phase shifts almost do not change when we ease our rejection criteria in that we also keep data that are within four standard deviations with respect to the other data. In that case we still have to reject more than 400 data, which are very much in disagreement with the other data in our database. The result of this analysis strengthens our belief that the 932 *np* data we reject are indeed statistically bad data and therefore that their rejection is valid.

We conclude this section with a remark regarding the very low-energy *np* data. The value for the *np* scattering cross section at "zero energy" σ_0, and the (n,p) coherent scattering length a_p can be expressed in terms of the singlet scattering length a_s and the triplet scattering length a_t according to

$$\sigma_0 = \pi(3a_t^2 + a_s^2) \ , \quad a_p = (3a_t + a_s)/4\mu \ . \tag{24}$$

Here $\mu = (1 + M_n/M_H)^{-1}$ with M_H the hydrogen mass. The two most recent experimental values for σ_0 are in disagreement with each other. Houk finds [43] $\sigma_0 = 20.436(23)$ b, whereas Dilg finds [44] $\sigma_0 = 20.491(14)$ b. Because these accurate values are within two standard deviations from each other, we cannot use our statistical criteria to decide which of these two measurements best fits in with the other *np* scattering data of our database (i.e., we

predict a value for σ_0 which lies somewhere in between these two experimental values). For that reason both measurements are included in the database. A more careful analysis of these two experiments will be deferred to the near future.

VI. RESULTS

If our model is correct and if the database constitutes a correct statistical ensemble, one expects for $N_{\rm df}$ degrees of freedom a $\chi^2_{\rm min}$ of

$$\langle \chi^2_{\rm min} \rangle / N_{\rm df} = 1 \pm \sqrt{2/N_{\rm df}} \ .$$

For all analyses presented in this paper, we find that $\chi^2_{\rm min}$ is about three standard deviations higher than the corresponding expectation value. This result implies that there is still room for improvements in our model and that the difference is at least partially due to small shortcomings in this model. We also determined the second and higher moments of the χ^2 distribution of our database and we find that they compare very favorably with their theoretical expectations. For more details regarding these statistical considerations, we refer to Ref. [4].

Before discussing some of the salient features of having such a good m.e. partial-wave solution, we will first present the detailed results of our energy-dependent (m.e.) and energy-independent (s.e.) *pp* and *np* analyses.

A. Energy-dependent analyses

Our first step in analyzing the *NN* scattering data was to redo the m.e. *pp* partial-wave analysis, now including the new analyzing-power data [38, 39, 40]. For the 1787 scattering data with 1613 degrees of freedom, we expect $\chi^2_{\rm min}/N_{\rm df} = 1.000 \pm 0.035$. We find $\chi^2_{\rm min}(pp) = 1787.0$, or $\chi^2/N_{\rm df} = 1.108$. The boundary-condition parameters which parametrize the lower partial waves are given in the upper half of Table III. These parameters c_n have dimension (MeV fm^{2n}) and are related to the coefficients a_n of Eq. (12) according to $c_n = a_n/2M_r$, with k^2 in units of fm^{-2}. For coupled channels we use the parametrization of Eq. (13), with θ in rad. The m.e. results for each group of data are practically the same as those from our previous *pp* analysis [1], so we will not reproduce Table I of that paper again. The χ^2 results for the three groups of new analyzing power data have been given in the previous section.

The *pp* phase shifts and mixing parameters of the lower partial waves with their statistical m.e. errors are listed in Table IV. Here and in the other tables, all *pp* phase shifts are the phase shifts of the electromagnetic plus nuclear interaction with respect to electromagnetic wave functions (δ^{EM}_{EM+N}, following the notation of Ref. [4]). They can easily be converted to phase shifts of the Coulomb plus nuclear interaction with respect to Coulomb wave functions (δ^{C1}_{C1+N}), which are the phase shifts one usually calculates, e.g., using potential models. For $l \neq 0$ we simply have $\delta^{EM}_{EM+N} \approx \delta^{C1}_{C1+N}$, whereas for the $^1S_0$ we have to use

$$^1S_0: \quad \delta^{EM}_{EM+N} \approx \delta^{C1}_{C1+N} + \widetilde{\Delta}_0 - \rho_0 - \tau_0 \ ,$$

where for details we refer to Ref. [4]. The errors given for the m.e. phase shifts are purely statistical, and are directly related to the uncertainty in the fitted boundary-condition parameters parametrizing these partial waves. They are rather small which can be understood from the fact that we need only 21 boundary-condition parameters to describe 1787 data.

For the analysis of the *np* scattering data the values for these m.e. *pp* phase shifts up to $J = 4$ (except for the $^1S_0$ phase shift) are used as input for the pion Coulomb corrections as described at the end of Sec. III B. These provide the m.e. values for the isovector *np* phase shifts. For the 2514 scattering data with 2332 degrees of freedom we expect $\chi^2_{\rm min}/N_{\rm df} = 1.000 \pm 0.029$. We find $\chi^2_{\rm min}(np) = 2489.2$, or $\chi^2/N_{\rm df} = 1.067$. The boundary-condition parameters are listed in the lower half of Table III. The m.e. results for each group of data are given in Table II. There we give the χ^2 values, the predicted normalization with which the experimental data should be multiplied before comparing them with the theoretical values, which data were rejected, and why they were rejected. The *np* $^1S_0$ and isoscalar phase shifts and mixing parameters which are parametrized by a boundary condition are listed in Table V. We do not give a m.e. error on the $^3G_4$ phase shift, because for this partial wave the boundary-condition does not contain any free adjustable parameters. The *np* isovector phase shifts (except the $^1S_0$) are given in Table VI. The values for the pion Coulomb corrections can be read off the tables by taking the difference between the *pp* phase shifts of Table IV and the corresponding *np* phase shifts of Table VI. These pion Coulomb corrections are very different from the corrections given by the VPI-SU analyses [11, 12] or the Graz prescription [17]. For example, in contrast with these latter two methods, in our analysis the ^3P *np* phase shifts are *smaller* than the corresponding *pp* phase shifts. The charge dependence in the $^1S_0$ partial wave is not due to a theoretically calculated pion Coulomb correction, but arises from the independent parametrizations used for the *pp* and *np* systems, respectively.

We have also performed a combined partial-wave analysis. In this analysis we simultaneously fit the *pp* as well as the *np* data, so the *pp* phase shifts will then change in such a way that the corresponding *np* phase shifts (as obtained via the pion Coulomb corrections) give rise to a drop in the total χ^2. To be specific, in the combined analysis the *pp* boundary-condition parameters are changed with the result that χ^2 on the *pp* data rises with $\Delta\chi^2 = 7.7$ from 1787.0 to 1794.7, but χ^2 on the *np* data drops with $\Delta\chi^2 = 20.1$ from 2489.2 to 2469.1. So the total χ^2 drops with $\Delta\chi^2 = 12.4$ from 4276.2 to 4263.8, and $\chi^2/N_{\rm df} = 1.081$. However, the rise in χ^2 on the *pp* data in the combined analysis, together with the fact that in our present approach the analysis of the *pp* data alone is less model dependent than the combined analysis, we believe that the phase shifts as obtained in the analysis of the *pp* data alone are closer to the "true" *pp* phase shifts. The differences between the phase shifts of the combined analysis and the two separate analyses are very small, but increase with increasing energies. To demonstrate the magnitude of these differences Tables IV–VI also contain the results from the combined analysis at 100, 200, and 300 MeV.

B. Energy-independent analyses

Although the energy-dependent analysis is far more superior than a set of energy-independent analyses (see the next section), we still decided to present the results of these

analyses for reasons of comparison and to illustrate the situation.

Our s.e. analyses are performed by only fitting the a_0 constant of Eq. (12) for each partial wave. The other boundary-condition parameters are held fixed at their m.e. values in order to ensure the proper local energy behavior. It is important to note that in that way we explicitly include the constraints provided by the m.e. solution: all phase shifts that are not fitted (i.e., the intermediate and higher partial waves) are kept at their m.e. values. In our s.e. analyses the data are clustered around ten energies from 382.54 keV (the interference minimum) up to 320 MeV. These analyses provide us with ten error matrices. The error matrix is the inverse of half the second-derivative matrix of the χ^2 hypersurface with respect to the phase shifts which are varied within that particular energy bin. These error matrices for the *pp*, the *np*, and the combined $pp + np$ analyses are available upon request. They can conveniently be used, for example, to make a quick comparison of the predictions of a potential model with the *NN* scattering data [158].

The energy-dependence in our m.e. solution of $V_S(k^2)$ for the *pp* $^3P_0$ partial wave is shown in Fig. 2(a). The black bullets with their error bars are the short-range potentials as obtained in the s.e. analyses. The large error bar at, e.g., $T_{\rm lab} = 25$ MeV reflects the fact that in a s.e. analysis at 25 MeV the *pp* $^3P_0$ phase shift cannot be determined very accurately. The s.e. result at 10 MeV is clearly off with respect to the m.e. curve. A similar discrepancy occurs in the $^3P_1$ partial wave (not shown). Apparently, some of the *pp* data around 10 MeV are not completely consistent with the other data in our database. This was already inferred from the results of one of our earlier, preliminary analyses [2]. This figure also nicely demonstrates that all s.e. results are statistically scattered around the m.e. solution (as they should). In Fig. 2(b) we show what the total potential for the $^3P_0$ partial wave looks like. The solid line is the value for the short-range potential corresponding to its value at $T_{\rm lab} = 200$ MeV and the dashed curve is the OPE potential, including the HBE contributions of the Nijmegen soft-core potential [10].

A similar picture for the *np* $^1P_1$ partial wave is shown in Fig 3. The s.e. short-range potentials for this partial wave at 25 and 100 MeV reflect the fact that the *np* data cannot pin down the $^1P_1$ partial wave at these energies, due to a lack of accurate differential cross-section data.

The lower partial-wave phase shifts are plotted in Figs. 4 and 5. The solid curves represent the results from the energy-dependent analyses, and the black dots denote the results form the energy-independent analyses with their errors. In Fig. 4 the isovector *np* phase shifts as given via the pion Coulomb corrections are represented by the dashed line. The *np* $^1S_0$ is parametrized independently of the *pp* $^1S_0$ and hence is shown separately in Fig. 5. The s.e. errors are the square roots of the diagonal elements of the error matrices.

Our s.e. values are statistically scattered around the curve representing the m.e. result, as they should. We also give the s.e. results from the 1992 VPI-SU solution VL40 which can be found in SAID [36], and from the 1992 analysis by Bugg and Bryan [23].

For most *pp* phase shifts the agreement is very good. A peculiar exception is the $^3P_0$ phase shift from the VPI-SU analysis at 75 MeV. The difference with our m.e. solution amounts to almost 6 standard deviations. For the isoscalar *np* phase shifts the spread in the results of the three different s.e. solutions (Nijmegen, VPI-SU, and Bugg) is larger, where the Nijmegen s.e. results are still close to the Nijmegen m.e. solution. The differences are at least partially due to the different treatments of fixing the *np* isovector phase shifts

(see Sec. III B). Other differences between these three analyses are in the treatment of the electromagnetic interaction and in the treatment of the higher partial waves.

Although for some phase shifts there appears to be a large difference between the three s.e. solutions, this does not truly reflect the uncertainty in these phase shifts. As already stressed before, the m.e. result provides the "best" value for the phase shift, and it can be determined very accurately.

The large values for the ε_1 mixing parameter of the VPI-SU solution at 50, 75, and 100 MeV are probably due to the fact that they do not remove the erroneous Harwell [85] and Uppsala [119] data. These data have a large influence on ε_1 as determined in an energy-independent analysis, whereas their influence in an energy-dependent analysis is much smaller. We do not find any evidence for a large ε_1 in our energy-dependent analysis. This is in disagreement with a recent claim based on the results of a set of s.e. analyses below 160 MeV [159]. But then this set of s.e. analyses is to a certain extent a kind of VPI-SU analysis: it uses the same computer code [36] and the same database (including some recent new data). It is not understandable that the results of these s.e. analyses were not compared with the results of a m.e. analysis, because this would have revealed that such large values for ε_1 can easily be ruled out.

C. Multi energy versus single energy

As already mentioned in the Introduction, the set of s.e. analyses requires many more fit parameters than the m.e. analysis covering the same energy region. As a representative example we here compare our m.e. and s.e. analyses of the NN data below 350 MeV. In our m.e. analysis of these data we need a total of 39 parameters to adequately describe the energy dependence of the phase shifts. Each additional parameter is superfluous in the sense that the statistical error on such a parameter turns out to be larger than the value of the parameter itself. Also the resulting drop in $\chi^2_{\rm min}$ is negligible. On the other hand, for the set of ten s.e. analyses covering the same energy range we have a total of 116 parameters. The difference of 77 additional parameters indicates that the set of s.e. analyses is strongly overparametrized and hence contains noise. Although the total χ^2 reached in the ten s.e. analyses is 180 less than the $\chi^2_{\rm min}$ reached in the m.e. analysis, this drop is only obtained at the expense of introducing 77 extra parameters (compared to the 39 parameters needed in the m.e. analysis).

Another shortcoming of doing s.e. analyses is that the data in the energy interval where the s.e. analysis is done can be such that they are very insensitive to variations in the value of one particular phase shift (e.g., the absence of np spin correlation data often implies that the ε_1 mixing parameter is ill determined). In that case that particular phase shift cannot reliably be determined in the s.e. analysis, whereas its value can be determined very accurately in the m.e. analysis (see below).

Similarly, it is possible that the energy interval we want to investigate in the s.e. partial-wave analysis contains an erroneous set of data, which can be described reasonably well by adjusting one of the phase shifts without affecting the description of the other data too much. That particular phase shift will then differ very much from its m.e. value, which makes this solution unacceptable. Not comparing with the results of the energy-dependent

analysis (and therefore, with the constraints imposed by all the other data) will not show the incorrectness of this solution. This can give rise to incorrect conclusions.

Because the $\chi^2_{\rm min}$ obtained in our energy-dependent analysis is so close to the theoretical expectation value, we believe that we have a unique solution, which is then also rather stable. The values for the phase shifts and for the theoretically calculated scattering observables as well as the statistical m.e. errors on these quantities are then essentially correct. When we include new data in the m.e. partial-wave analysis, the phase shifts are not expected to change by more than one or two m.e. standard deviations. So the values and errors determined in the m.e. analysis are much more stable than those determined in the s.e. analysis. In two cases we will demonstrate this.

Recently, very accurate *pp* analyzing-power data at 50.04 MeV [38, 42] have become available, as well as an *np* longitudinal total cross section [110] and a set of *np* spin-correlation data at 67.5 MeV [112]. These experiments were expected to pin down the *NN* phase shifts around 50 MeV much more accurately. Let us see, what influence these experiments had on our m.e. solution. The 50.04 MeV *pp* A_y data mainly affect the tensor (T) and spin-orbit (LS) combinations of the ^3P phase shifts. Without the new 50.04 MeV data our m.e. values for these phase shifts at 50 MeV are

$$\Delta_T = -3.745^\circ(22) \quad \text{and} \quad \Delta_{LS} = 2.601^\circ(34) \ ,$$

whereas with these data included they read

$$\Delta_T = -3.733^\circ(12) \quad \text{and} \quad \Delta_{LS} = 2.606^\circ(21) \ .$$

In the s.e. analysis covering the 50 MeV region these phase shifts change from

$$\Delta_T = -3.759^\circ(43) \quad \text{and} \quad \Delta_{LS} = 2.509^\circ(87) \ ,$$

to

$$\Delta_T = -3.741^\circ(14) \quad \text{and} \quad \Delta_{LS} = 2.592^\circ(28) \ ,$$

when the 50.04 MeV data are included. Similarly, the 67.5 MeV A_{zz} and $\Delta\sigma_L$ data mainly affect the $^1P_1$ phase shift and ε_1 mixing parameter. Without the new data our m.e. values for these phase shifts at 50 MeV are

$$\delta(^1P_1) = -9.78^\circ(11) \quad \text{and} \quad \varepsilon_1 = 2.15^\circ(7) \ ,$$

whereas with these data included we get

$$\delta(^1P_1) = -9.67^\circ(8) \quad \text{and} \quad \varepsilon_1 = 2.11^\circ(5) \ .$$

The influence of these data in the s.e. analysis of the *np* data covering the 50 MeV region is much more pronounced. Without these new data there are no *np* data around 50 MeV that pin down the ε_1 mixing parameter. As a consequence, it has the unrealistic high value of $\varepsilon_1 = 5.69^\circ(64)$ and rules of statistics do not apply anymore. The statistical errors on the s.e. phase parameters are much too small and the actual errors should be amended with large (unknown) systematic errors. Inclusion of the 67.5 MeV data improves the s.e. analysis

considerably and we find $\varepsilon_1 = 2.57°(36)$, in good agreement with the m.e. analysis. From these examples we see that our m.e. solution is very stable when we add these accurate new data, whereas the same is not necessarily true for the phase shifts as determined in a s.e. analysis.

Similarly, we investigated that the inclusion of the still unpublished data by the Erlangen [31, 32] and Karlsruhe [33] groups does not change the m.e. values for the phase shifts by more than one or two standard deviations.

D. Normalizations

The fact that the m.e. phase shifts can be determined very accurately also implies that angular dependences of cross sections, analyzing powers, spin correlation parameters, etc., are fixed rather well. As a consequence, the normalization on a particular group of such data can be determined very accurately in the m.e. analysis. In almost all cases our determination of the normalization is (much) more accurate than the uncertainty quoted by the experimentalists. An illustrative exception once again involves the 50.04 MeV *pp* analyzing-power data. Originally these ten A_y data were presented with a 2% normalization uncertainty [38]. When we assume that the normalization for these data is unknown (i.e., we leave the normalization as a free parameter), we find in the m.e. analysis $N_{\rm fl,1} = 1.0150(71)$, which is consistent with, but more accurate than, the experimental determination of $N_{\rm ex,1} = 1.00(2)$. Including this latter experimental value we find $N_{\rm th,1} = 1.0133(67)$. Later in a separate experiment [42] there was a new determination of the normalization, yielding $N_{\rm ex,2} = 1.0069(39)$. When we compare this with our determination $N_{\rm fl,1}$ we see again the consistency, but now the error in $N_{\rm ex,2}$ is smaller than our error in $N_{\rm fl,1}$. Renormalizing the original A_y data with this factor 1.0069 and including the new scale uncertainty of 0.39%, we determine our new normalization to be $N_{\rm th,2} = 1.0019(34)$, which is in excellent agreement with the determination by the experimentalists.

One should realize, however, that this very accurate experimental determination of the normalization is only applicable at a small selected set of energies (for details, see Refs. [39, 42]). At any other energy, it is extremely difficult or even impossible to achieve this high accuracy, whereas our m.e. analysis provides an accurate determination of the normalization of any group of data at any arbitrary energy below 350 MeV. This has important consequences. For instance, in case of differential cross-section measurements it is only the shape that is really of importance, and it is not necessary to go through the experimentally very difficult procedure of determining the absolute normalization to a high accuracy. This was already demonstrated in an earlier paper by our group [24], where we discussed the 11 sets of differential cross sections by Bonner *et al.* [133], where the measurements below 300 MeV have a free normalization, whereas the measurements above 300 MeV have a finite normalization uncertainty of 4%. There we showed that in our m.e. analysis the normalization for each set can be determined with an accuracy of 0.7%. There is almost no difference between the sets with a free normalization and the sets with the 4% normalization uncertainty.

Even in the extreme case where *all* groups of data are given a free normalization, we can still determine the normalizations very accurately, where the errors are only slightly larger.

VII. SUMMARY

We have performed m.e. partial-wave analyses on the *pp* data, on the *np* data, and on the combined database including the *pp* as well as the *np* data. For the *pp* analysis we find $\chi^2_{\rm min}(pp) = 1787.0$ for 1787 scattering data with 1613 degrees of freedom. The *np* analysis yields $\chi^2_{\rm min}(np) = 2489.2$ for 2514 scattering data with 2332 degrees of freedom. The combined $pp + np$ analysis yields $\chi^2_{\rm min} = 4263.8$ for 4301 scattering data with 3945 degrees of freedom, where the *pp* data contribute $\chi^2(pp) = 1794.7$ and the *np* data $\chi^2(np) = 2469.1$. All three analyses have an excellent $\chi^2/N_{\rm data} \approx 1$, which is significantly lower than any other m.e. partial-wave analysis we know of.

In these m.e. analyses all lower partial-wave phase shifts are accurately known. Hence, the results of any s.e. analysis should always be compared with this (or any other high-quality) m.e. analysis in order to judge whether or not the resulting s.e. phase shifts are realistic. Our energy-dependent solution is expected to be very stable under the inclusion of new experiments. Consequently, we can give very accurate predictions of all *NN* scattering data at any angle and at any energy below 350 MeV. We have to make a proviso, however. Since we do not include any constraints on the energy behavior of the phase shifts beyond 350 MeV, the results at the high end of our energy range ($T_{\rm lab} \gtrsim 325$ MeV) may be somewhat less reliable. A first indication for this shows up in the preliminary results of a *pp* analysis of all data up to 500 MeV, which includes inelasticities [160]. The χ^2 on the 300–350 MeV data in this latter analysis is somewhat higher than in the analysis presented in this paper. We believe that the results for the phase shifts obtained in the 0–500 MeV analysis are closer to the "true" values, because now the energy dependence near 350 MeV is not only dictated by the data below 350 MeV.

An advantage of having an accurate m.e. solution is that the normalization on a group of differential cross sections, analyzing powers, or spin correlation parameters can be determined very accurately. There is no impediment in only measuring the angular distribution of, e.g., the differential cross section and to forgo the experimentally much more difficult determination of the absolute normalization. However, we are still in need of more accurate data. For instance, around 10 MeV there are inconsistencies between the *pp* scattering data, whereas in the 100 MeV region the quality and variety of both *pp* and *np* data is very poor. Moreover, in order to be able to do an analysis of the *np* data, we had to resort to some particular assumptions to provide us with the isovector phase shifts. An independent analysis of the *np* data, parametrizing the isoscalar as well as the isovector partial waves, is under investigation. However, because of the large number of partial waves to be parametrized, it is still rather difficult to perform such an analysis and it would be very helpful to have more high-accuracy *np* experiments at our disposal.

Finally, we mention that for the $^3S_1$-$^3D_1$ coupled channel, we can also easily extrapolate the energy dependence to the deuteron pole. In that way we are able to extract some of the deuteron parameters from the scattering data. Preliminary results using this method have been published some years ago, when we analyzed the *np* scattering data below 30 MeV [161]. A detailed account of the determination of the deuteron parameters and the other low-energy parameters using the energy dependence as given by our present m.e. analysis will be left to a future paper. Here we only quote the result of this extrapolation which yields $B = 2.2247(35)$ MeV for the deuteron binding energy. This is in excellent

agreement with the experimental determination [162] of $B = 2.224\,575(9)$ MeV.

ACKNOWLEDGMENTS

We would like to thank the other members of our group for many valuable discussions. Part of this work was included in the research program of the Stichting voor Fundamenteel Onderzoek der Materie (FOM) with financial support from the Nederlandse Organisatie voor Wetenschappelijk Onderzoek (NWO).

REFERENCES

[1] J.R. Bergervoet, P.C. van Campen, R.A.M. Klomp, J.-L. de Kok, T.A. Rijken, V.G.J. Stoks, and J.J. de Swart, Phys. Rev. C **41**, 1435 (1990).
[2] R.A.M. Klomp, V.G.J. Stoks, and J.J. de Swart, Phys. Rev. C **42**, R1258 (1991).
[3] R.A.M. Klomp, V.G.J. Stoks, and J.J. de Swart, Phys. Rev. C **45**, 2023 (1992).
[4] J.R. Bergervoet, P.C. van Campen, W.A. van der Sanden, and J.J. de Swart, Phys. Rev. C **38**, 15 (1988).
[5] R.L. Jaffe and F.E. Low, Phys. Rev. D **19**, 2105 (1979).
[6] G.J.M. Austen and J.J. de Swart, Phys. Rev. Lett. **50**, 2039 (1983).
[7] V.G.J. Stoks and J.J. de Swart, Phys. Rev. C **42**, 1235 (1990).
[8] L. Durand III, Phys. Rev. **108**, 1597 (1957).
[9] G. Breit, Phys. Rev. **99**, 1581 (1955).
[10] M.M. Nagels, T.A. Rijken, and J.J. de Swart, Phys. Rev. D **17**, 768 (1978).
[11] R.A. Arndt, L.D. Roper, R.A. Bryan, R.B. Clark, B.J. VerWest, and P. Signell, Phys. Rev. D **28**, 97 (1983).
[12] R.A. Arndt, J.S. Hyslop III, and L.D. Roper, Phys. Rev. D **35**, 128 (1987).
[13] R.A. Arndt, L.D. Roper, R.L. Workman, and M.W. McNaughton, Phys. Rev. D **45**, 3995 (1992).
[14] J.J. de Swart, J.R.M. Bergervoet, P.C.M. van Campen, and W.A.M. van der Sanden, Lecture Notes in Physics Vol. 236 (Springer, Berlin, 1985), p. 179.
[15] V.G.J.M. Stoks, Ph. D. thesis, University of Nijmegen, 1990.
[16] R.A. Arndt (private communication).
[17] J. Fröhlich, L. Streit, H. Zankel, and H. Zingl, J. Phys. G **6**, 841 (1980).
[18] J. Fröhlich, L. Streit, and H. Zankel, Phys. Lett. **92B**, 8 (1980).
[19] J. Fröhlich and H. Zankel, Phys. Lett. **82B**, 173 (1979).
[20] D.V. Bugg, J.A. Edgington, C. Amsler, R.C. Brown, C.J. Oram, K. Shakarchi, N.M. Stewart, G.A. Ludgate, A.S. Clough, D. Axen, S. Jaccard, and J. Vávra, J. Phys. G **4**, 1025 (1978).
[21] R. Dubois, D. Axen, R. Keeler, M. Comyn, G.A. Ludgate, J.R. Richardson, N.M. Stewart, A.S. Clough, D.V. Bugg, and J.A. Edgington, Nucl. Phys. **A377**, 554 (1982).
[22] D.V. Bugg, Phys. Rev. C **41**, 2708 (1990).
[23] D.V. Bugg and R.A. Bryan, Nucl. Phys. **A540**, 449 (1992).
[24] V. Stoks, R. Timmermans, and J.J. de Swart, Phys. Rev. C **47**, 512 (1993).
[25] V.G.J. Stoks, R.A.M. Klomp, and J.J. de Swart, unpublished.
[26] M. Lacombe, B. Loiseau, J.M. Richard, R. Vinh Mau, J. Côté, P. Pirès, and R. de Tourreil, Phys. Rev. C **21**, 861 (1980).
[27] J. Bystricky, F. Lehar, and P. Winternitz, J. Phys. (Paris) **39**, 1 (1978).
[28] P. La France and P. Winternitz, J. Phys. (Paris) **41**, 1391 (1980).
[29] A. Gersten, Nucl. Phys. **A290**, 445 (1977); A. Gersten, Phys. Rev. C **18**, 2252 (1978).
[30] G.J.M. Austen, Ph. D. thesis, University of Nijmegen, 1982.
[31] W. Kretschmer *et al.*, in *Book of Contributions, XIth International Conference on Few-Body Systems in Particle and Nuclear Physics*, Tokyo/Sendai, 1986, edited by T. Sasakawa *et al.* (Tohoku University, Sendai, 1986), p. 442; W. Schuster, Habilitationsschrift, University of Erlangen, 1989 (unpublished).

[32] W. Kretschmer *et al.*, in Contributed Papers to the XIIth International Conference on Few-Body Problems in Physics, Vancouver, 1989, edited by B.K. Jennings, TRIUMF Report No. TRI-89-2, C12.
[33] P. Doll *et al.*, in Contributed Papers to the XIIth International Conference on Few-Body Problems in Physics, Vancouver, 1989, edited by B.K. Jennings, TRIUMF Report No. TRI-89-2, C16.
[34] J. Bystricky and F. Lehar, in *Physics Data*, edited by H. Behrens and G. Ebel (Fachinformationszentrum, Karlsruhe, Federal Republic of Germany, 1978), Vol. 11-1.
[35] J. Bystricky and F. Lehar, in *Physics Data*, edited by H. Behrens and G. Ebel (Fachinformationszentrum, Karlsruhe, Federal Republic of Germany, 1981), Vol. 11-3.
[36] Scattering Analysis Interactive Dial-up (SAID), Virginia Polytechnic Institute, Blacksburg, Virginia (R.A. Arndt, private communication).
[37] P. Kroll, in *Physics Data*, edited by H. Behrens and G. Ebel (Fachinformationszentrum, Karlsruhe, Federal Republic of Germany, 1981), Vol. 22-1.
[38] J. Smyrski *et al.*, Nucl. Phys. **A501** (1989) 319.
[39] B. von Przewoski *et al.*, Phys. Rev. C **44**, 44 (1991).
[40] W.K. Pitts *et al.*, Phys. Rev. C **45**, R1 (1992); W.K. Pitts, *ibid.*, **45**, 455 (1992).
[41] V.G.J. Stoks and J.J. de Swart, Nucl. Phys. **A514**, 309 (1990).
[42] A. Converse *et al.*, Phys. Rev. C **45**, 2320 (1992).
[43] T.L. Houk, Phys. Rev. C **3**, 1886 (1971).
[44] W. Dilg, Phys. Rev. C **11**, 103 (1975).
[45] L. Koester and W. Nistler, Z. Phys. A **272**, 189 (1975).
[46] Y. Fujita, K. Kobayashi, T. Oosaki, and R.C. Block, Nucl. Phys. **A258**, 1 (1976).
[47] W.D. Allen and A.T.G. Ferguson, Proc. Phys. Soc. London, Sect. A **68**, 1077 (1955).
[48] C.E. Engelke, R.E. Benenson, E. Melkonian, and J.M. Lebowitz, Phys. Rev. **129**, 324 (1963).
[49] P.J. Clements and A. Langsford, Phys. Lett. **30B**, 25 (1969).
[50] J.C. Davis and H.H. Barschall, Phys. Rev. C **3**, 1798 (1971).
[51] J.C. Davis *et al.*, Phys. Rev. C **4**, 1061 (1971).
[52] Gy. Hrehuss and T. Czibók, Phys. Lett. **28B**, 585 (1969).
[53] A. Bratenahl, J.M. Peterson, and J.P. Stoering, Phys. Rev. **110**, 927 (1958).
[54] G.J. Weisel *et al.*, Phys. Rev. C **46**, 1599 (1992).
[55] D. Holslin, J. McAninch, P.A. Quin, and W. Haeberli, Phys. Rev. Lett. **61**, 1561 (1988).
[56] G.S. Mutchler and J.E. Simmons, Phys. Rev. C **4**, 67 (1971).
[57] W. Tornow, P.W. Lisowski, R.C. Byrd, and R.L. Walter, Phys. Rev. Lett. **39**, 915 (1977); Nucl. Phys. **A340**, 34 (1980).
[58] M. Schöberl *et al.*, Nucl. Phys. **A489**, 284 (1988).
[59] J. Arvieux and J. Pouxe, Phys. Lett. **32B**, 468 (1970).
[60] M. Schöberl *et al.*, J. Phys. G **10**, L247 (1984).
[61] E. Greiner and H. Karge, Ann. Phys. (Leipzig) **16**, 354 (1965).
[62] T. Nakamura, J. Phys. Soc. Jpn. **15**, 1359 (1960).
[63] J.D. Seagrave, Phys. Rev. **97**, 757 (1955).
[64] A. Suhami and R. Fox, Phys. Lett. **24B**, 173 (1967).
[65] M. Tanaka, N. Koori, and S. Shirato, J. Phys. Soc. Jpn. **28**, 11 (1970).
[66] J.E. Brock *et al.*, Nucl. Phys. **A361**, 368 (1981).

[67] R. Fischer *et al.*, Nucl. Phys. **A282**, 189 (1977).
[68] W.T. Morton, Proc. Phys. Soc. London **91**, 899 (1967).
[69] P.H. Bowen *et al.*, Nucl. Phys. **22**, 640 (1961).
[70] R. Garrett *et al.*, Nucl. Phys. **A196**, 421 (1972).
[71] W. Benenson, R.L. Walter, and T.H. May, Phys. Rev. Lett. **8**, 66 (1962).
[72] D.T.L. Jones and F.D. Brooks, Nucl. Phys. **A222**, 79 (1974).
[73] C.L. Morris, T.K. O'Malley, J.W. May, Jr., and S.T. Thornton, Phys. Rev. C **9**, 924 (1974).
[74] W. Tornow *et al.*, Phys. Rev. C **37**, 2326 (1988).
[75] J. Wilczynski *et al.*, Nucl. Phys. **A425**, 458 (1984).
[76] M. Ockenfels *et al.*, Nucl. Phys. **A534**, 248 (1991).
[77] J.M. Peterson, A. Bratenahl, and J.P. Stoering, Phys. Rev. **120**, 521 (1960).
[78] A. Galonsky and J.P. Judish, Phys. Rev. **100**, 121 (1955).
[79] D.E. Groce and B.D. Sowerby, Nucl. Phys. **83**, 199 (1966).
[80] R.B. Day, R.L. Mills, J.E. Perry, Jr., and F. Scherb, Phys. Rev. **114**, 209 (1959).
[81] A. Langsford *et al.*, Nucl. Phys. **74**, 241 (1965); preliminary data published by P.H. Bowen *et al.*, Phys. Rev. Lett. **7**, 248 (1961).
[82] B.R.S. Simpson and F.D. Brooks, Nucl. Phys. **A505**, 361 (1989).
[83] G. Fink *et al.*, Nucl. Phys. **A518**, 561 (1990).
[84] E.R. Flynn and P.J. Bendt, Phys. Rev. **128**, 1268 (1962).
[85] J.P. Scanlon *et al.*, Nucl. Phys. **41**, 401 (1963).
[86] J.J. Malanify, P.J. Bendt, T.R. Roberts, and J.E. Simmons, Phys. Rev. Lett. **17**, 481 (1966).
[87] R.B. Perkins and J.E. Simmons, Phys. Rev. **130**, 272 (1963).
[88] J.E. Simmons, Rev. Mod. Phys. **39**, 542 (1967).
[89] T.W. Burrows, Phys. Rev. C **7**, 1306 (1973).
[90] G.E. Bohannon, T. Burt, and P. Signell, Phys. Rev. C **13**, 1816 (1976).
[91] L.N. Rothenberg, Phys. Rev. C **1**, 1226 (1970).
[92] T.G. Masterson, Phys. Rev. C **6**, 690 (1972).
[93] F.P. Brady *et al.*, Phys. Rev. Lett. **25**, 1628 (1970).
[94] J. Sromicki *et al.*, Phys. Rev. Lett. **57**, 2359 (1986).
[95] M. Drosg and D.M. Drake, Nucl. Instrum. Methods **160**, 143 (1979).
[96] T.C. Montgomery *et al.*, Phys. Rev. Lett. **31**, 640 (1973); Phys. Rev. C **16**, 499 (1977).
[97] M. Ockenfels *et al.*, Nucl. Phys. **A526**, 109 (1991).
[98] A. Bol *et al.*, Phys. Rev. C **32**, 623 (1985).
[99] R.A. Eldred, B.E. Bonner, and T.A. Cahill, Phys. Rev. C **12**, 1717 (1975).
[100] N. Ryu *et al.*, Nucl. Phys. **A180**, 657 (1972).
[101] P.W. Lisowski *et al.*, Phys. Rev. Lett. **49**, 255 (1982).
[102] A. Bol *et al.*, Phys. Rev. C **32**, 308 (1985).
[103] D.H. Fitzgerald *et al.*, Phys. Rev. C **21**, 1190 (1980).
[104] R. Garrett *et al.*, Phys. Rev. C **21**, 1149 (1980).
[105] J.L. Romero *et al.*, Phys. Rev. C **17**, 468 (1978).
[106] S.W. Johnsen *et al.*, Phys. Rev. Lett. **38**, 1123 (1977).
[107] A.J. Bersbach, R.E. Mischke, and T.J. Devlin, Phys. Rev. D **13**, 535 (1976).
[108] R.A. Arndt, J. Binstock, and R.A. Bryan, Phys. Rev. D **8**, 1397 (1973).

[109] N.S.P. King *et al.*, Phys. Rev. C **21**, 1185 (1980).
[110] P. Haffter *et al.*, Nucl. Phys. **A548**, 29 (1992).
[111] C. Brogli-Gysin *et al.*, Nucl. Phys. **A541**, 137 (1992).
[112] M. Hammans *et al.*, Phys. Rev. Lett. **66**, 2293 (1991).
[113] C. Whitehead, S. Tornabene, and G.H. Stafford, Proc. Phys. Soc. London **75**, 345 (1960).
[114] D.F. Measday and J.N. Palmieri, Nucl. Phys. **85**, 142 (1966).
[115] C.Y. Chih and W.M. Powell, Phys. Rev. **106**, 539 (1957).
[116] V. Culler and R.W. Waniek, Phys. Rev. **99**, 740 (1955).
[117] G.H. Stafford, C. Whitehead, and P. Hillman, Nuovo Cimento **5**, 1589 (1957).
[118] T.C. Griffith, A.P. Banford, M.Y. Uppal, and W.S.C. Williams, Proc. Phys. Soc. London, Sect. A **71**, 305 (1958).
[119] T. Rönnqvist *et al.*, Phys. Rev. C **45**, R496 (1992).
[120] P. Hillman and G.H. Stafford, Nuovo Cimento **3**, 633 (1956).
[121] J.J. Thresher, R.G.P. Voss, and R. Wilson, Proc. Roy. Soc. London, Sect. A **229**, 492 (1955).
[122] M.W. Shapiro, A.M. Cormack, and A.M. Koehler, Phys. Rev. **138**, B823 (1965).
[123] V. Grundies, J. Franz, E. Rössle, and H. Schmitt, Phys. Lett. **158B**, 15 (1985).
[124] A.S. Carroll, P.M. Patel, N. Strax, and D. Miller, Phys. Rev. **134**, B595 (1964).
[125] R.K. Hobbie and D. Miller, Phys. Rev. **120**, 2201 (1960).
[126] W.G. Collins, Jr., and D.G. Miller Phys. Rev. **134**, B575 (1964).
[127] P.M. Patel, A. Carroll, N. Strax, and D. Miller, Phys. Rev. Lett. **8**, 491 (1962).
[128] V.J. Howard *et al.*, Nucl. Phys. **A218**, 140 (1974).
[129] D.F. Measday, Phys. Rev. **142**, 584 (1966).
[130] T.C. Randle *et al.*, Proc. Phys. Soc. London, Sect. A **69**, 760 (1956).
[131] G.H. Stafford and C. Whitehead, Proc. Phys. Soc. **79**, 430 (1962).
[132] J.N. Palmieri and J.P. Wolfe, Phys. Rev. C **3**, 144 (1971).
[133] B.E. Bonner *et al.*, Phys. Rev. Lett. **41**, 1200 (1978).
[134] R. Binz *et al.*, Nucl. Phys. **A533**, 601 (1991).
[135] J. Sowinski *et al.*, Phys. Lett. **199B**, 341 (1987).
[136] P.F. Shepard, T.J. Devlin, R.E. Mischke, and J. Solomon, Phys. Rev. D **10**, 2735 (1974).
[137] A.R. Thomas, D. Spalding, and E.H. Thorndike, Phys. Rev. **167**, 1240 (1968).
[138] Yu.M. Kazarinov and Yu.N. Simonov, Zh. Eksp. Teor. Fiz. **43**, 35 (1962) [Sov. Phys.–JETP **16**, 24 (1963)].
[139] W. Hürster *et al.*, Phys. Lett. **90B**, 367 (1980).
[140] R.K. Keeler *et al.*, Nucl. Phys. **A377**, 529 (1982).
[141] D. Bandyopadhyay *et al.*, Phys. Rev. C **40**, 2684 (1989).
[142] A.S. Clough *et al.*, Phys. Rev. C **21**, 988 (1980).
[143] D. Axen *et al.*, Phys. Rev. C **21**, 998 (1980).
[144] C. Amsler *et al.*, Nucl. Instrum. Methods **144**, 401 (1977).
[145] T.J. Devlin *et al.*, Phys. Rev. D **8**, 136 (1973).
[146] D. Cheng, B. Macdonald, J.A. Helland, and P.M. Ogden, Phys. Rev. **163**, 1470 (1967).
[147] O. Chamberlain *et al.*, Phys. Rev. **105**, 288 (1957).
[148] C. Amsler *et al.*, Phys. Lett. **69B**, 419 (1977).

[149] A. Ashmore *et al.*, Nucl. Phys. **36**, 258 (1962).
[150] R.T. Siegel, A.J. Hartzler, and W.A. Love, Phys. Rev. **101**, 838 (1956).
[151] J.C. Davis and H.H. Barschall, Phys. Lett. **27B**, 636 (1968).
[152] M.H. MacGregor, R.A. Arndt, and R.M. Wright, Phys. Rev. **173**, 1272 (1968).
[153] R.B. Schwartz, R.A. Schrack, and H.T. Heaton, Phys. Lett. **30B**, 36 (1969).
[154] S. Cierjacks *et al.*, Phys. Rev. Lett. **23**, 866 (1969).
[155] J.M. Clement, P. Stoler, C.A. Goulding, and R.W. Fairchild, Nucl. Phys. **A183**, 51 (1972).
[156] J. Binstock and R. Bryan, Phys. Rev. D **9**, 2528 (1974); R.A. Arndt, J. Binstock, and R. Bryan, *ibid.* **8**, 1397 (1973); R. Bryan and J. Binstock, *ibid.* **10**, 72 (1974); P.F. Brady, in Lecture Notes in Physics Vol. 82, edited by H. Zingl, M. Haftel, and H. Zankel (Springer-Verlag, Berlin, 1978), p. 137.
[157] N. Olsson (private communication).
[158] V. Stoks and J.J. de Swart, Phys. Rev. C **47**, 761 (1993).
[159] R. Henneck, Phys. Rev. C **47**, 1859 (1993).
[160] J.-L. de Kok, Ph. D. thesis, University of Nijmegen, 1993.
[161] V.G.J. Stoks, P.C. van Campen, W. Spit, and J.J. de Swart, Phys. Rev. Lett. **60**, 1932 (1988).
[162] C. van der Leun and C. Alderliesten, Nucl. Phys. **A380**, 261 (1982).

TABLES

TABLE I. Effects on the phase shifts due to the removal of the Coulomb interaction (next to last column) and subsequently including the pion-mass differences in the OPE potential (last column). Phase shifts are in degrees.

$T_{\rm lab}$	Partial wave	With Coulomb	Coulomb removed	Pion-mass difference
10 MeV	$^3P_0$	3.860	4.231	3.784
	$^3P_1$	–2.049	–2.235	–2.052
	$^3P_2$	0.642	0.734	0.699
	$^1D_2$	0.164	0.178	0.155
25 MeV	$^3P_0$	9.007	9.349	8.564
	$^3P_1$	–4.905	–5.126	–4.851
	$^3P_2$	2.445	2.629	2.514
	$^1D_2$	0.685	0.716	0.670
50 MeV	$^3P_0$	12.215	12.334	11.438
	$^3P_1$	–8.275	–8.508	–8.211
	$^3P_2$	5.721	5.974	5.753
	$^1D_2$	1.686	1.735	1.701

TABLE II. Data reference table. A dagger denotes data not included in the nucleon-nucleon scattering data tables (Refs. [34, 35]). An asterisk denotes data not included in the data set NN931 of SAID (Ref. [36]).

$T_{\rm lab}$(MeV)	No.[a], type	χ^2	% error	Pred. norm[b]	Reject	Ref.	Comment	Institute
0.0	2 σ_0	4.36	None			[43, 44]		
0.0	1 a_p	0.01	None			[45]		
0.023645†	1 $\sigma_{\rm tot}$	2.70	None			[46]		Kyoto
0.060–0.550*	5 $\sigma_{\rm tot}$	2.42	None			[47]		Harwell
0.4926–3.186	2 $\sigma_{\rm tot}$	0.91	None			[48]	c	Columbia
0.841–19.957	17 $\sigma_{\rm tot}$	19.26	None		1.161 MeV, 9.885 MeV	[49]	d	Harwell
1.500–27.515	27 $\sigma_{\rm tot}$	22.37	None			[50]		Madison
2.535	1 $\sigma_{\rm tot}$	3.78	None			[51]		Madison
2.72	2 σ	0.59	3.7	1.009(36)	170.0°	[52]	e	Budapest
3.01	2 σ	2.80	3.7	1.023(36)	170.0°	[52]	e	Budapest
3.33	3 σ	1.72	3.7	1.011(29)	170.0°	[52]	e	Budapest
3.69	4 σ	1.70	3.7	1.023(25)	170.0°	[52]	e	Budapest
4.01	4 σ	0.66	3.7	1.011(26)	170.0°	[52]	e	Budapest
4.34	4 σ	2.70	3.7	1.021(20)	170.0°	[52]	e	Budapest
4.65	4 σ	2.82	3.7	1.030(22)	170.0°	[52]	e	Budapest
4.91	4 σ	1.30	3.7	1.036(19)	170.0°	[52]	e	Budapest
5.10	4 σ	4.35	3.7	1.056(19)	170.0°	[52]	e	Budapest
5.24	4 σ	6.19	3.7	1.062(18)	170.0°	[52]	e	Budapest
7.17–14.02	6 $\sigma_{\rm tot}$	15.12	None			[53]		Liverpool
7.6†	4 P	10.82	3.0	1.016(28)		[54]		TUNL
10.03†	12 P	10.53	4.0	0.969(25)		[55]		Madison
11.0	1 P	0.04	3.5	0.999(35)		[56]		Los Alamos
12.0†	8 P	19.07	3.0	1.054(24)		[54]		TUNL
13.5†	1 P	0.02	3.0	0.999(28)		[57]		TUNL
13.7†	1 A_{yy}	6.66	None			[58]		Erlangen
14.0	3 σ	17.89	None		All	[59]	f	Grenoble
14.0†	1 A_{yy}	1.99	None			[60]		Erlangen
14.1	6 σ	2.32	Float[g]	0.546(9)	70.0°	[61]	e,h	Jena
14.1	4 σ	2.58	0.73	0.992(4)		[62]		Kyoto
14.1	6 σ	1.70	4.0	1.041(11)		[63]	d	Los Alamos
14.1	17 σ	11.66	None		14.0°	[64]	d,i	Haifa
14.1	8 σ	12.51	None			[65]		Tokyo
14.1	10 P	3.94	3.0	1.001(27)		[66]		Auckland
14.1†	5 P	5.31	3.0	1.034(24)		[54]		TUNL
14.5	8 P	8.46	None			[67]		Hamburg
14.8†	1 P	0.54	3.0	1.008(29)		[57]		TUNL
15.7	16 σ	11.06	Float[g]	48.9(6)		[68]		Glasgow
15.8–111.5	63 $\sigma_{\rm tot}$	67.07	2.0	1.035(4)		[69]		Harwell
16.0†	1 P	0.01	3.0	0.999(28)		[57]		TUNL
16.0†	5 P	6.53	3.0	0.989(22)		[54]		TUNL
16.2	3 P	0.54	None			[70]		Auckland
16.4	3 P	2.77	9.3	1.00(9)		[71]		Madison
16.4	4 P	1.81	None			[72]	j	Cape Town
16.8	1 P	0.02	4.4	0.999(43)		[56]		Los Alamos
16.9	4 P	3.70	6.0	1.062(49)		[73]		Virginia
16.9†	11 P	15.87	3.0	1.024(22)		[74]		TUNL
16.9†	4 P	0.33	3.0	1.001(30)		[74]		TUNL
17.0†	6 P	3.76	2.1	0.999(21)		[75]		Karlsruhe
17.4†	1 D_t	2.05	None			[76]		Bonn
17.8–29.0	5 $\sigma_{\rm tot}$	6.62	None			[77]		Liverpool
17.9	11 σ	16.29	1.9	1.038(8)		[78]	e	Oak Ridge
18.5†	4 P	2.57	3.0	0.998(25)		[54]		TUNL
19.0†	6 P	4.28	3.0	1.003(29)		[75]		Karlsruhe
19.565–27.950	3 $\sigma_{\rm tot}$	2.70	None			[79]		Canberra
19.665	1 $\sigma_{\rm tot}$	0.30	None			[80]		Los Alamos
20.5	9 P	7.02	18.8	0.89(13)		[81]		Harwell
21.1	6 P	5.40	3.0	1.020(25)		[73]		Virginia
21.6	7 P	1.57	None			[72]	k	Cape Town
21.6†	5 P	5.69	4.0	0.967(33)		[82]		Cape Town
22.0†	8 P	12.65	3.1	0.967(23)		[75]		Karlsruhe

22.2†	5 σ	1.70	1.0	1.002(2)		[83]		Karlsruhe
22.5	12 σ	8.45	None			[84]		Los Alamos
22.5	6 σ	3.05	3.3		All	[85]	l	Harwell
23.1	2 P	0.33	12.2	1.02(12)		[56, 86]		Los Alamos
23.1	2 P	0.50	3.5	1.005(31)		[56]		Los Alamos
23.1	6 P	3.11	7.7	1.02(6)		[87]		Los Alamos
23.1	4 A_{yy}	0.45	12.2	0.99(10)		[86, 88]		Los Alamos
23.7	4 P	1.49	10.9	1.05(11)		[71]		Madison
24.0	3 σ	2.90	1.2	0.989(8)		[89, 90]		Madison
24.0	4 σ	17.97	0.43		All	[91]	f	Madison
24.0	2 σ	0.45	None			[92]		Madison
24.63–59.35	8 σ_{tot}	9.14	0.3	1.002(2)		[93]		Davis
25.0†	5 σ	5.58	1.0	1.010(2)		[83]		Karlsruhe
25.0†	16 P	22.84	3.3	1.061(11)		[94]		Madison
25.0†	8 P	7.31	2.9	0.972(19)		[75]		Karlsruhe
25.30–31.06†	2 σ	0.24	None			[95]		Los Alamos
25.5†	1 D_t	0.06	None			[76]		Bonn
25.8	8 σ	5.07	3.0	1.013(10)		[96]		Davis
25.8	8 σ	3.78	3.0	1.006(6)		[96]		Davis
25.8†	1 D_t	3.98	None			[97]		Bonn
26.9–72.5†	5 σ_{tot}	4.05	None			[98]		Leuven
27.2	4 σ	1.37	1.3	0.995(9)		[89, 90]		Madison
27.4†	5 σ	6.27	1.0	1.008(3)		[83]		Karlsruhe
27.5	11 σ	23.80	2.5		All	[85]	l	Harwell
27.5†	8 P	6.72	3.0	0.974(20)	151.4°	[75]		Karlsruhe
29.6	11 P	2.06	None		All	[99]	m	Davis
29.6	3 P	1.31	10.0	0.96(6)		[56]		Los Alamos
29.9†	5 σ	3.47	1.0	1.004(3)		[83]		Karlsruhe
30.0	12 P	14.16	8.33	1.06(8)		[81]		Harwell
30.0†	8 P	4.42	2.9	0.997(19)		[75]		Karlsruhe
31.6	2 P	2.30	None			[100]		Hiroshima
32.5	1 P	1.06	None			[100]		Hiroshima
32.5	15 σ	41.06	2.1		All	[85]	f,l	Harwell
32.9†	6 σ	14.05	1.0	1.005(3)		[83]		Karlsruhe
33.0†	8 P	7.49	2.9	0.964(18)		[75]		Karlsruhe
35.8†	6 σ	16.99	1.0	0.990(4)		[83]		Karlsruhe
36.0†	8 P	8.12	2.9	0.961(19)		[75]		Karlsruhe
37.5	17 σ	33.23	1.8		All	[85]	f,l	Harwell
39.0–350.0†	70 σ_{tot}	56.77	1.0	1.006(3)		[101]	e,n	Los Alamos
39.7†	6 σ	21.62	1.0		All	[83]	f	Karlsruhe
40.0†	2 σ	2.49	None			[102]		Leuven
40.0	15 P	11.65	6.02	0.956(41)		[81]		Harwell
40.0†	8 P	13.46	2.9	0.977(20)		[75]		Karlsruhe
42.5	22 σ	47.61	1.8		All	[85]	f,l	Harwell
45.0†	2 σ	0.48	None			[102]		Leuven
47.5	22 σ	53.28	1.7		All	[85]	f,l	Harwell
50.0†	2 σ	0.11	None			[102]		Leuven
50.0†	6 σ	17.14	1.0	1.021(5)		[83]		Karlsruhe
50.0	8 σ	5.37	3.0	0.994(10)		[96]		Davis
50.0	12 σ	10.66	3.0	1.027(5)		[96]		Davis
50.0	4 P	0.91	None			[103]		Davis
50.0	4 P	0.35	None			[103]		Davis
50.0	7 P	3.98	3.6	0.995(29)	120.6°	[104]		Davis
50.0	16 P	15.45	4.79	0.978(28)		[81]		Harwell
50.0	9 P	8.93	3.6	1.048(26)		[105]		Davis
50.0†	8 P	15.33	3.4	0.945(20)		[75]		Karlsruhe
50.0	4 A_{yy}	3.50	7.9	1.07(8)		[103]		Davis
50.0	4 A_{yy}	2.22	25.0	1.34(26)		[106]		Davis
52.5	23 σ	43.71	1.7		All	[85]	f,l	Harwell
55.1†	2 σ	0.71	None			[102]		Leuven
57.5	23 σ	48.67	1.8		All	[85]	f,l	Harwell
58.8	9 σ	5.86	10.0	1.058(16)		[107]		Princeton
60.0	16 P	23.56	3.89	1.096(26)		[81]		Harwell
60.9	9 σ	7.98	Float[g]	1.156(11)		[108]		Oak Ridge
61.0†	1 σ	0.03	None			[102]		Leuven
62.2†	2 σ	2.46	None			[102]		Leuven
62.5	23 σ	68.39	1.7		All	[85]	f,l	Harwell

63.1	19 σ	28.72	Float[g]	1.038(6)	86.2°, 159.7°, 165.8°	[109]		Los Alamos
65.0[†]	2 σ	0.17	None			[102]		Leuven
66.0[†*]	1 $\Delta\sigma_{\mathrm{L}}$	1.50	6.0	1.064(40)		[110]		PSI
67.5	11 σ	9.81	10.0	1.075(17)	49.5°	[107]		Princeton
67.5[†]	12 P	9.35	4.0	0.988(10)		[111]		PSI
67.5[†]	19 P	24.14	4.0	1.044(10)		[111]		PSI
67.5[†]	20 A_{zz}	15.57	6.0	1.032(15)		[112]		PSI
70.0[†]	2 σ	0.89	None			[102]		Leuven
70.0	24 σ	102.5	1.4		All	[85]	f,l	Harwell
70.0	16 P	24.73	3.90	1.117(27)		[81]		Harwell
76.2[†]	1 σ	2.75	None			[102]		Leuven
76.7	11 σ	9.26	10.0	1.109(17)	49.6°	[107]		Princeton
77.0[*]	17 P	101.2	7.6		All	[113]	f	Harwell
80.0	24 σ	50.73	1.5		All	[85]	f,l	Harwell
80.0	16 P	10.13	4.23	1.055(26)		[81]		Harwell
86.5	11 σ	20.44	10.0	1.180(19)		[107]		Princeton
88.2–150.9	7 σ_{tot}	0.32	None		All	[114]	m	Harvard
89.5	24 σ	32.35	1.6		All	[85]	f,l	Harwell
90.0	18 σ	24.41	Float[g]	1.102(17)	145.0°	[115]		Berkeley
90.0	16 P	10.58	5.12	1.058(35)		[81]		Harwell
93.4–106.8	4 σ_{tot}	1.82	None			[116]		Harvard
95.0	15 P	32.59	8.0	1.076(41)		[117]		Harwell
96.0	4 σ	0.60	None			[118]		London
96.0[†]	32 σ	114.2	4.0		All	[119]	f,l	Uppsala
96.8	11 σ	17.10	10.0	1.117(19)		[107]		Princeton
98.0	9 P	5.83	14.3	1.09(13)		[120]		Harwell
99.0	24 σ	36.01	1.7		All	[85]	f,l	Harwell
100.0	16 P	7.28	7.31	0.970(44)		[81]		Harwell
105.0	7 σ	2.33	8.0	0.913(23)		[121]		Oxford
107.6	11 σ	18.61	10.0	1.094(19)		[107]		Princeton
108.5	24 σ	33.88	1.8		All	[85]	f,l	Harwell
110.0	16 P	18.86	10.03	0.96(6)		[81]		Harwell
118.8	11 σ	15.52	10.0	1.102(21)		[107]		Princeton
120.0	16 P	8.16	14.9	0.97(9)		[81]		Harwell
125.0–168.0	2 σ_{tot}	3.64	12.0	1.20(9)		[122]		Harvard
125.9–344.5[†]	12 σ_{tot}	3.27	1.5	1.007(5)		[123]	e,n	SIN
126.0	6 P	5.66	4.1	0.969(27)		[124]		Harvard
128.0	10 σ	3.00	7.0	1.031(12)		[125]		Harvard
128.0	10 P	11.76	8.0	1.017(45)		[125]		Harvard
128.0	1 D_t	0.01	None			[126]		Harvard
128.0	5 D_t	9.29	8.0	1.02(8)		[127]		Harvard
129.0	9 σ	5.03	16.0	0.997(49)		[128]		Harwell
129.0	16 σ	8.55	7.0	1.028(7)		[128]		Harwell
129.0	15 σ	11.83	6.5	1.058(11)		[129]	o	Harvard
130.0	14 σ	11.97	4.0	1.051(25)		[130]		Harwell
130.5	11 σ	13.87	10.0	1.059(15)		[107]		Princeton
137.0	5 σ	9.59	None			[118]		London
137.0	7 σ	4.29	10.0	1.078(32)		[121]		Oxford
140.0	14 P	25.69	4.4	1.046(21)		[131]		Harwell
142.8	11 σ	3.96	10.0	1.038(13)		[107]		Princeton
150.0	16 σ	8.61	6.5	1.039(8)		[129]	o	Harvard
152.0[†]	13 σ	162.6	None		All	[132]	f	Harvard
155.4	11 σ	25.48	10.0	1.073(15)	39.5°	[107]		Princeton
162.0	43 σ	63.00	Float[g]	1.092(7)		[133]	d	Los Alamos
168.5	11 σ	14.51	10.0	1.077(16)	39.6°	[107]		Princeton
177.9	44 σ	46.51	Float[g]	1.083(7)		[133]	d	Los Alamos
180.0–332.0[†]	4 $\Delta\sigma_{\mathrm{L}}$	0.97	4.3	0.980(35)		[134]		SIN
180.0–332.0[†]	4 $\Delta\sigma_{\mathrm{T}}$	1.55	12.4	0.95(10)		[134]		SIN
181.0[†]	10 P	9.15	4.0	1.010(15)	119.6°	[135]		Bloomington
181.0[†]	10 A_{yy}	8.41	8.0	0.970(13)		[135]		Bloomington
181.8	11 σ	14.94	10.0	1.114(18)		[107]		Princeton
182.0[*]	14 σ	11.37	(8.0)		All	[136]	f,l	Princeton
194.5	42 σ	76.11	Float[g]		All	[133]	d,f	Los Alamos
195.6	11 σ	20.20	10.0	1.060(18)		[107]		Princeton
196.0[*]	16 σ	48.57	(5.5)		All	[136]	f,l	Princeton
199.0	7 σ	9.94	2.1	0.965(9)	86.6°, 96.3°	[137]		Rochester

199.0	8 P	25.38	10.0		All	[137]	f	Rochester
200.0	1 σ_{tot}	0.15	None			[138]		JINR
200.0	21 σ	53.85	2.1		All	[137, 138]	f	JINR
200.0*	31 σ	182.2	Float[g]		All	[139]	d,p	SIN
210.0	11 σ	13.02	10.0	1.039(20)		[107]		Princeton
210.0*	16 σ	42.84	(3.6)		All	[136]	f,l	Princeton
211.5	43 σ	31.35	Float[g]	1.063(7)		[133]	d	Los Alamos
212.0–319.0	3 σ_{tot}	0.39	(0.8)	0.954(7)		[140]	n	TRIUMF
212.0	4 σ	0.51	2.0	0.996(12)		[140]		TRIUMF
212.0	39 σ	44.01	3.2	1.008(4)	88.57°, 90.45°, 92.34°, 94.29°	[140]		TRIUMF
220.0*	33 σ	221.2	Float[g]		All	[139]	d,p	SIN
220.0†	16 P	17.51	3.5	0.997(19)		[141]		TRIUMF
220.0†	16 P	13.17	2.5	0.982(16)	144.18°	[141]		TRIUMF
220.0	16 P	21.62	3.0	1.023(24)		[142]	q	TRIUMF
220.0†	16 A_{yy}	8.16	5.5	1.032(13)		[141]		TRIUMF
220.0	10 D_t	8.27	3.0	1.001(30)		[142]	q	TRIUMF
220.0	7 A_t	12.23	3.0	0.997(29)		[143]	q	TRIUMF
220.0	7 R_t	15.04	3.0	1.071(25)		[143]	q	TRIUMF
220.0*	1 R_t, 1 R'_t	1.59	None			[144]		TRIUMF
224.0*	16 σ	70.82	(3.2)		All	[136]	f,l	Princeton
224.3	11 σ	11.19	10.0	0.996(21)		[107]		Princeton
229.1	49 σ	64.62	Float[g]	1.058(7)		[133]	d	Los Alamos
239.0*	18 σ	45.98	(3.1)		All	[136]	f,l	Princeton
239.5	11 σ	5.43	10.0	1.085(27)		[107]		Princeton
240.0*	34 σ	313.3	Float[g]		All	[139]	d,p	SIN
247.2–344.3	4 σ_{tot}	56.11	0.09		All	[145]	f,n	Princeton
247.2	53 σ	38.94	Float[g]	1.042(7)		[133]	d	Los Alamos
257.0*	19 σ	89.60	(3.0)		All	[136]	f,l	Princeton
260.0*	35 σ	250.1	Float[g]		All	[139]	d,p	SIN
265.8	63 σ	59.13	Float[g]	1.029(6)		[133]	d	Los Alamos
267.2	11 σ	6.49	10.0	1.011(20)	11.4°	[107]		Princeton
280.0*	35 σ	244.8	Float[g]		All	[139]	d,p	SIN
284.0*	19 σ	114.3	(8.0)		All	[136]	f,l	Princeton
284.8	73 σ	79.64	Float[g]	1.053(5)		[133]	d	Los Alamos
300.0*	35 σ	194.7	Float[g]		All	[139]	d,p	SIN
304.2	79 σ	79.87	4.0	1.003(4)		[133]	d	Los Alamos
307.0	8 P	13.03	3.0	1.004(24)	47.8°	[146]		Berkeley
309.6	11 σ	13.38	10.0	0.929(28)		[107]		Princeton
310.0	19 P	27.44	7.2	1.007(36)	53.4°, 147.7°	[147]		Berkeley
313.0*	19 σ	88.86	(2.4)		All	[136]	f,l	Princeton
319.0	7 σ	3.40	(2.0)	0.917(12)		[140]		TRIUMF
319.0	64 σ	77.84	3.9	1.007(3)		[140]		TRIUMF
320.0*	36 σ	150.1	Float[g]		All	[139]	d,p	SIN
324.1	81 σ	92.15	4.0	1.057(5)		[133]	d	Los Alamos
325.0	42 P	54.11	12.0	0.905(14)	45.0°, 50.0°, 55.0°, 60.0°	[148]	d	TRIUMF
325.0†	19 P	12.73	3.1	0.984(16)		[141]		TRIUMF
325.0†	19 P	15.58	2.5	0.978(14)		[141]		TRIUMF
325.0	21 P	29.17	3.0	1.020(14)	44.99°, 50.08°, 60.31°, 118.39°	[142]	r	TRIUMF
325.0†	19 A_{yy}	25.05	5.3	0.965(24)		[141]		TRIUMF
325.0	12 D_t	11.98	3.0	1.010(30)		[142]	r	TRIUMF
325.0	9 A_t	7.13	3.0	1.013(27)	153.5°	[143]	r	TRIUMF
325.0	9 R_t	14.87	3.0	1.002(23)		[143]	r	TRIUMF
325.0*	1 R_t, 1 R'_t	2.25	None			[144]		TRIUMF
325.0	8 D_t	4.27	12.0	1.00(11)		[148]	d	TRIUMF
340.0*	37 σ	174.6	Float[g]		All	[139]	d,p	SIN
343.0*	4 R_t	5.73	None			[144]		TRIUMF
343.8	11 σ	13.16	10.0	0.991(40)		[107]		Princeton
344.0*	21 σ	82.07	(2.1)		All	[136]	f,l	Princeton
344.3	80 σ	74.53	4.0	1.035(5)	131.51°	[133]	d	Los Alamos
350.0	10 σ	17.18	Float[g]	0.968(6)		[149]		Liverpool
350.0	7 σ	6.20	Float[g]	0.974(7)		[149]		Liverpool
350.0	12 P	6.85	4.3	0.992(31)	46.35° 85.12°, 126.13°	[150]		Pittsburgh

[a]The number includes all published data.
[b]Predicted norm with which the experimental values should be multiplied before comparison with the theoretical values.
[c]Adjustment of the original experimental energy of 3.205 MeV to 3.186 MeV according to Davis and Barschall [151].
[d]Numerical values were taken from the nucleon-nucleon scattering data tables [34].
[e]Numerical values were taken from the Brookhaven National Laboratory database.
[f]Rejected due to improbably high χ^2 (rejection criteria).
[g]Floated normalization because these data are relative only.
[h]Datum at 70.0° rejected as suggested by the authors (see Ref. [61]).
[i]Datum at 14.0° rejected in accordance with the suggestion by MacGregor, Arndt, and Wright [152].
[j]Renormalized by a factor of 0.76 according to Brock *et al.* [66].
[k]Renormalized by a factor of 0.84 according to Simpson and Brooks [82].
[l]Disagreement between single-group fit and multienergy fit too large.
[m]Rejected due to improbably low χ^2 (rejection criteria).
[n]Part of a group of data with points with $T_{\rm lab} > 350$ MeV.
[o]Data are those normalized to the Yale phase-shift analysis YLAN4M (see Ref. [129]).
[p]Forward-angle data sequentially rejected, so total group rejected.
[q]Renormalized by a factor of 0.974 according to Dubois *et al.* [21].
[r]Renormalized by a factor of 1.028 according to Dubois *et al.* [21].

TABLE III. Boundary-condition parameters for the lower partial waves. The upper half refers to the parameters used in the *pp* analysis, and the lower half to the parameters used in the *np* analysis. The coefficients c_n are in MeV fm^{2n} and correspond to $a_n/2M_r$ of Eq. (12).

	c_0	c_1	c_2	c_3
$^1S_0(pp)$	–15.003	0.174	3.074	–0.180
$^3P_0$	58.325	–6.430	2.119	0
$^3P_1$	64.926	5.082	0	0
$^1D_2$	61.420	–15.678	0	0
$P_a(J=2)$	–24.221	–0.112	–0.371	0
$\theta(J=2)$	0.015	0.013	0	0
$P_b(J=2)$	29.998	0	0	0
$^3F_3$	–18.794	0	0	0
$P_a(J=4)$	–79.252	13.768	0	0
$\theta(J=4)$	0	0	0	0
$P_b(J=4)$	0	0	0	0
$^1G_4$	466.566	0	0	0
$^1S_0(np)$	–17.813	–1.016	2.564	0
$^1P_1$	139.438	–23.412	2.479	0
$P_a(J=1)$	–40.955	4.714	1.779	0
$\theta(J=1)$	–0.370	0.009	0	0
$P_b(J=1)$	155.090	–12.053	0	0
$^3D_2$	–16.902	–3.506	0	0
$^1F_3$	248.730	0	0	0
$P_a(J=3)$	7.468	0	0	0
$\theta(J=3)$	–0.223	0	0	0
$P_b(J=3)$	0	0	0	0
$^3G_4$	0	0	0	0

TABLE IV. *pp* isovector phase shifts and their multienergy error in degrees as obtained in the multienergy *pp* analysis. Errors smaller than 0.0005° are not shown. The lower part lists the phase shifts as obtained in the combined $pp + np$ analysis.

$T_{\rm lab}$	$^1S_0$	$^1D_2$	$^1G_4$	$^3P_0$	$^3P_1$	$^3F_3$	$^3P_2$	ε_2	$^3F_2$	$^3F_4$	ε_4	$^3H_4$
1	32.684	0.001	0.000	0.134	–0.081	–0.000	0.014	–0.001	0.000	0.000	–0.000	0.000
	±0.005											
5	54.832	0.043	0.000	1.582	–0.902	–0.005	0.214	–0.052	0.002	0.000	–0.000	0.000
	±0.017			±0.006	±0.001		±0.001					
10	55.219	0.165	0.003	3.729	–2.060	–0.032	0.651	–0.200	0.013	0.001	–0.004	0.000
	±0.025			±0.017	±0.002		±0.002					
25	48.672	0.696	0.040	8.575	–4.932	–0.231	2.491	–0.810	0.105	0.020	–0.049	0.004
	±0.039	±0.001		±0.053	±0.008		±0.008	±0.001				
50	38.899	1.711	0.152	11.47	–8.317	–0.690	5.855	–1.712	0.338	0.108	–0.195	0.026
	±0.049	±0.004		±0.09	±0.017		±0.016	±0.004		±0.001		
100	24.97	3.790	0.418	9.45	–13.258	–1.517	11.013	–2.659	0.817	0.478	–0.539	0.108
	±0.08	±0.018	±0.001	±0.11	±0.032	±0.003	±0.025	±0.017	±0.004	±0.007		
150	14.75	5.606	0.700	4.74	–17.434	–2.100	13.982	–2.873	1.197	1.032	–0.849	0.211
	±0.13	±0.033	±0.003	±0.14	±0.045	±0.010	±0.039	±0.029	±0.014	±0.022		
200	6.55	7.058	0.993	–0.37	–21.25	–2.487	15.63	–2.759	1.424	1.678	–1.108	0.321
	±0.16	±0.045	±0.010	±0.17	±0.07	±0.025	±0.052	±0.037	±0.034	±0.039		
250	–0.31	8.27	1.272	–5.43	–24.77	–2.724	16.59	–2.542	1.47	2.325	–1.314	0.428
	±0.18	±0.06	±0.024	±0.21	±0.12	±0.049	±0.07	±0.046	±0.06	±0.051		
300	–6.15	9.42	1.503	–10.39	–27.99	–2.84	17.17	–2.34	1.34	2.89	–1.47	0.526
	±0.25	±0.08	±0.048	±0.33	±0.19	±0.11	±0.10	±0.09	±0.11	±0.06		
350	–11.13	10.69	1.64	–15.30	–30.89	–2.87	17.54	–2.21	1.04	3.30	–1.588	0.608
	±0.46	±0.14	±0.08	±0.57	±0.27	±0.13	±0.15	±0.11	±0.16	±0.11	±0.001	
100	24.97	3.782	0.418	9.55	–13.245	–1.518	11.013	–2.654	0.816	0.471	–0.539	0.108
	±0.08	±0.017		±0.09	±0.030	±0.002	±0.021	±0.016	±0.003	±0.006		
200	6.55	7.039	0.993	–0.27	–21.18	–2.499	15.65	–2.731	1.414	1.656	–1.107	0.321
	±0.16	±0.043	±0.008	±0.17	±0.06	±0.021	±0.05	±0.035	±0.029	±0.034		
300	–6.22	9.42	1.501	–10.44	–27.80	–2.89	17.15	–2.27	1.30	2.95	–1.473	0.526
	±0.23	±0.08	±0.040	±0.29	±0.16	±0.07	±0.09	±0.06	±0.09	±0.05		

TABLE V. $np\ ^1S_0$ and isoscalar phase shifts and their multienergy error in degrees as obtained in the multienergy np analysis. Errors smaller than 0.0005° are not shown. The lower part lists the phase shifts as obtained in the combined $pp + np$ analysis.

$T_{\rm lab}$	$^1S_0$	$^1P_1$	$^1F_3$	$^3D_2$	$^3G_4$	$^3S_1$	ε_1	$^3D_1$	$^3D_3$	ε_3	$^3G_3$
1	62.068	–0.187	–0.000	0.006	0.000	147.747	0.105	–0.005	0.000	0.000	–0.000
	±0.030					±0.010	±0.001				
5	63.63	–1.487	–0.011	0.222	0.001	118.178	0.672	–0.183	0.002	0.013	–0.000
	±0.08	±0.004				±0.021	±0.004				
10	59.96	–3.039	–0.066	0.846	0.014	102.611	1.159	–0.677	0.006	0.081	–0.004
	±0.11	±0.012				±0.035	±0.010	±0.001			
25	50.90	–6.311	–0.415	3.708	0.169	80.63	1.793	–2.799	0.048	0.549	–0.053
	±0.19	±0.039		±0.003		±0.07	±0.025	±0.006			
50	40.54	–9.67	–1.101	8.966	0.716	62.77	2.109	–6.433	0.324	1.600	–0.258
	±0.28	±0.08		±0.017		±0.10	±0.048	±0.017	±0.003		
100	26.78	–14.52	–2.089	17.28	2.154	43.23	2.42	–12.23	1.457	3.469	–0.934
	±0.38	±0.14	±0.003	±0.06		±0.14	±0.09	±0.05	±0.014	±0.002	
150	16.94	–18.65	–2.702	22.13	3.618	30.72	2.75	–16.48	2.736	4.804	–1.737
	±0.41	±0.16	±0.011	±0.10		±0.14	±0.11	±0.09	±0.033	±0.008	
200	8.94	–22.18	–3.235	24.51	4.987	21.22	3.13	–19.71	3.74	5.723	–2.534
	±0.39	±0.18	±0.027	±0.11		±0.15	±0.12	±0.14	±0.06	±0.020	±0.001
250	1.96	–25.13	–3.88	25.40	6.232	13.39	3.56	–22.21	4.37	6.357	–3.265
	±0.37	±0.20	±0.05	±0.11		±0.17	±0.13	±0.16	±0.09	±0.037	±0.001
300	–4.46	–27.58	–4.72	25.45	7.337	6.60	4.03	–24.14	4.62	6.80	–3.902
	±0.43	±0.22	±0.08	±0.12		±0.23	±0.17	±0.18	±0.12	±0.06	±0.004
350	–10.59	–29.66	–5.80	25.08	8.294	0.502	4.57	–25.57	4.60	7.13	–4.440
	±0.62	±0.33	±0.12	±0.19		±0.32	±0.25	±0.30	±0.16	±0.09	±0.007
100	26.71	–14.55	–2.090	17.27	2.154	43.19	2.42	–12.22	1.451	3.469	–0.934
	±0.38	±0.14	±0.004	±0.07		±0.14	±0.09	±0.05	±0.016	±0.003	
200	8.80	–22.19	–3.246	24.47	4.987	21.28	3.19	–19.73	3.72	5.730	–2.534
	±0.42	±0.20	±0.037	±0.12		±0.16	±0.13	±0.14	±0.07	±0.023	±0.001
300	–4.68	–27.51	–4.75	25.38	7.337	6.82	4.18	–24.27	4.58	6.83	–3.903
	±0.55	±0.28	±0.11	±0.16		±0.27	±0.20	±0.21	±0.14	±0.07	±0.004

TABLE VI. np isovector phase shifts in degrees as obtained via the pion Coulomb corrections in the multienergy np analysis. The lower part lists the phase shifts as obtained in the combined $pp + np$ analysis.

$T_{\rm lab}$	$^1D_2$	$^1G_4$	$^3P_0$	$^3P_1$	$^3F_3$	$^3P_2$	ε_2	$^3F_2$	$^3F_4$	ε_4	$^3H_4$
1	0.00	0.00	0.18	–0.11	–0.00	0.02	–0.00	0.00	0.00	–0.00	0.00
5	0.04	0.00	1.63	–0.94	–0.00	0.25	–0.05	0.00	0.00	–0.00	0.00
10	0.16	0.00	3.65	–2.06	–0.03	0.71	–0.18	0.01	0.00	–0.00	0.00
25	0.68	0.03	8.13	–4.88	–0.20	2.56	–0.76	0.09	0.02	–0.04	0.00
50	1.73	0.13	10.70	–8.25	–0.62	5.89	–1.63	0.30	0.10	–0.17	0.02
100	3.90	0.39	8.46	–13.24	–1.41	10.94	–2.58	0.76	0.45	–0.49	0.09
150	5.79	0.68	3.69	–17.46	–1.98	13.84	–2.80	1.12	0.99	–0.79	0.19
200	7.29	0.98	–1.44	–21.30	–2.36	15.46	–2.70	1.33	1.63	–1.05	0.29
250	8.53	1.28	–6.51	–24.84	–2.60	16.39	–2.49	1.35	2.26	–1.26	0.39
300	9.69	1.52	–11.47	–28.07	–2.73	16.95	–2.30	1.19	2.81	–1.42	0.48
350	10.96	1.67	–16.39	–30.97	–2.76	17.31	–2.18	0.87	3.21	–1.54	0.56
100	3.89	0.39	8.55	–13.22	–1.41	10.94	–2.57	0.76	0.44	–0.49	0.09
200	7.27	0.98	–1.34	–21.23	–2.37	15.47	–2.67	1.32	1.60	–1.05	0.29
300	9.69	1.52	–11.53	–27.88	–2.77	16.93	–2.23	1.16	2.88	–1.42	0.48

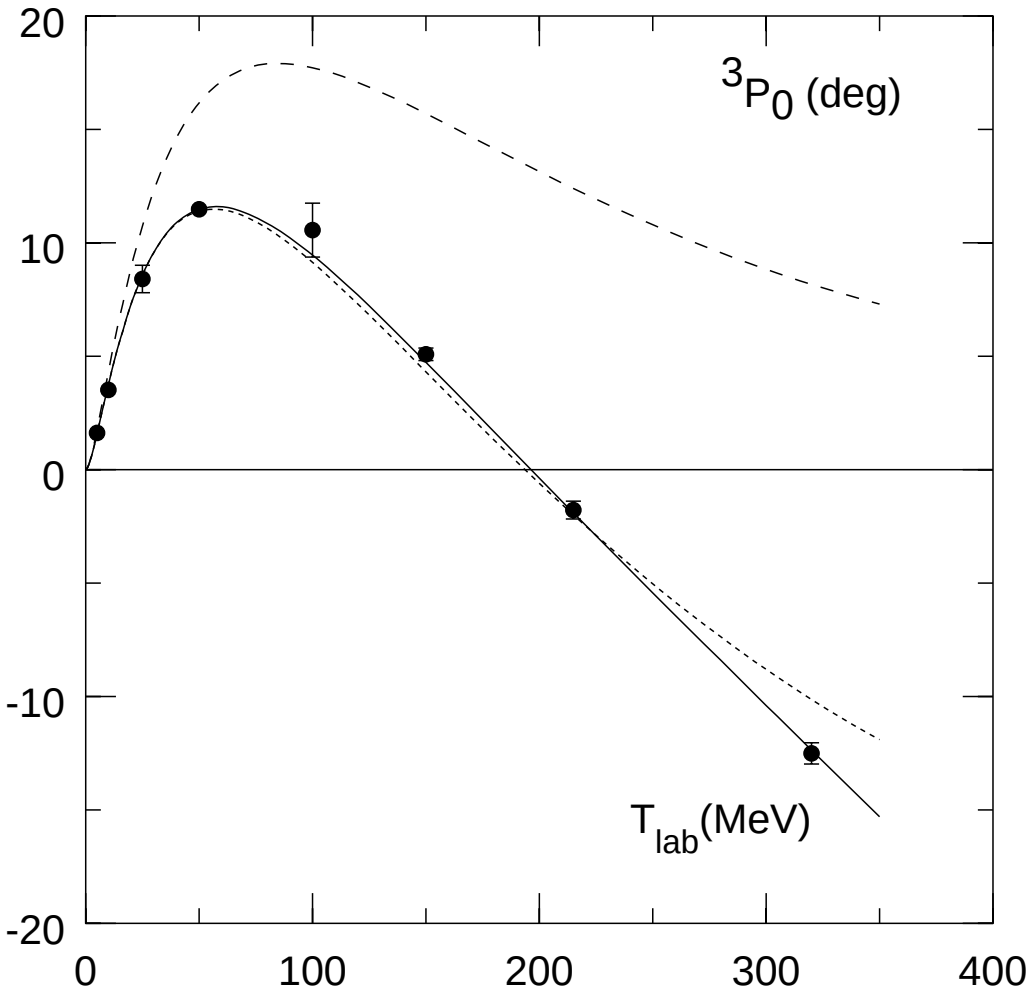

FIG. 1. Energy dependence of the pp $^3P_0$ phase shift using no parameters (dashed curve) or one parameter (dotted curve) in the short-range potential V_S. The solid curve represents the multienergy solution, which requires three parameters in V_S.

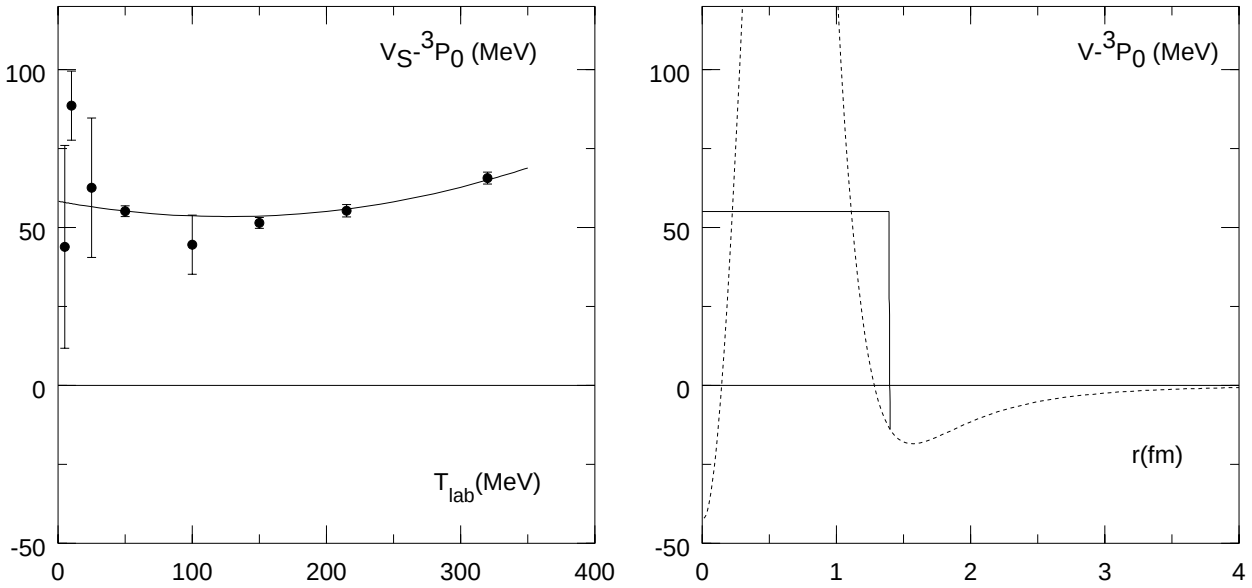

FIG. 2. (a) Energy dependence of V_S for the pp $^3P_0$ partial wave (solid curve). The bullets represent the values for V_S as obtained in the single-energy analyses. (b) The total potential in the pp $^3P_0$ partial wave. The solid line is the value for V_S at $T_{\rm lab} = 200$ MeV, and the dashed curve is the OPE potential, including the heavier-boson-exchange contributions of the Nijmegen potential [10].

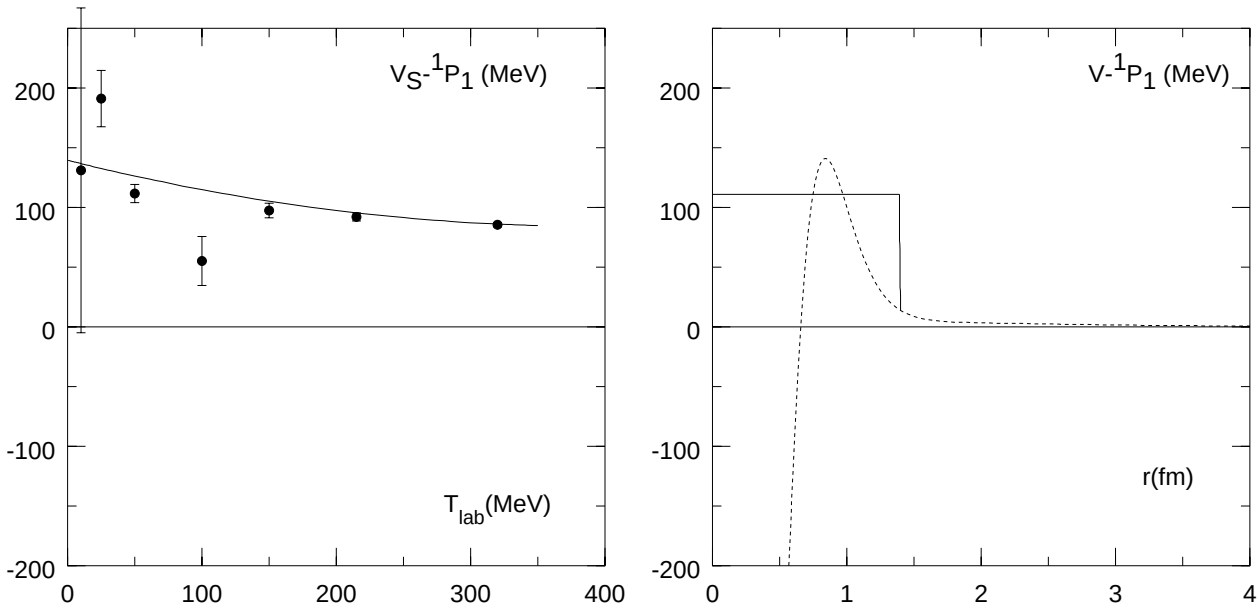

FIG. 3. Same as Fig. 2 but for the np $^1P_1$ partial wave.

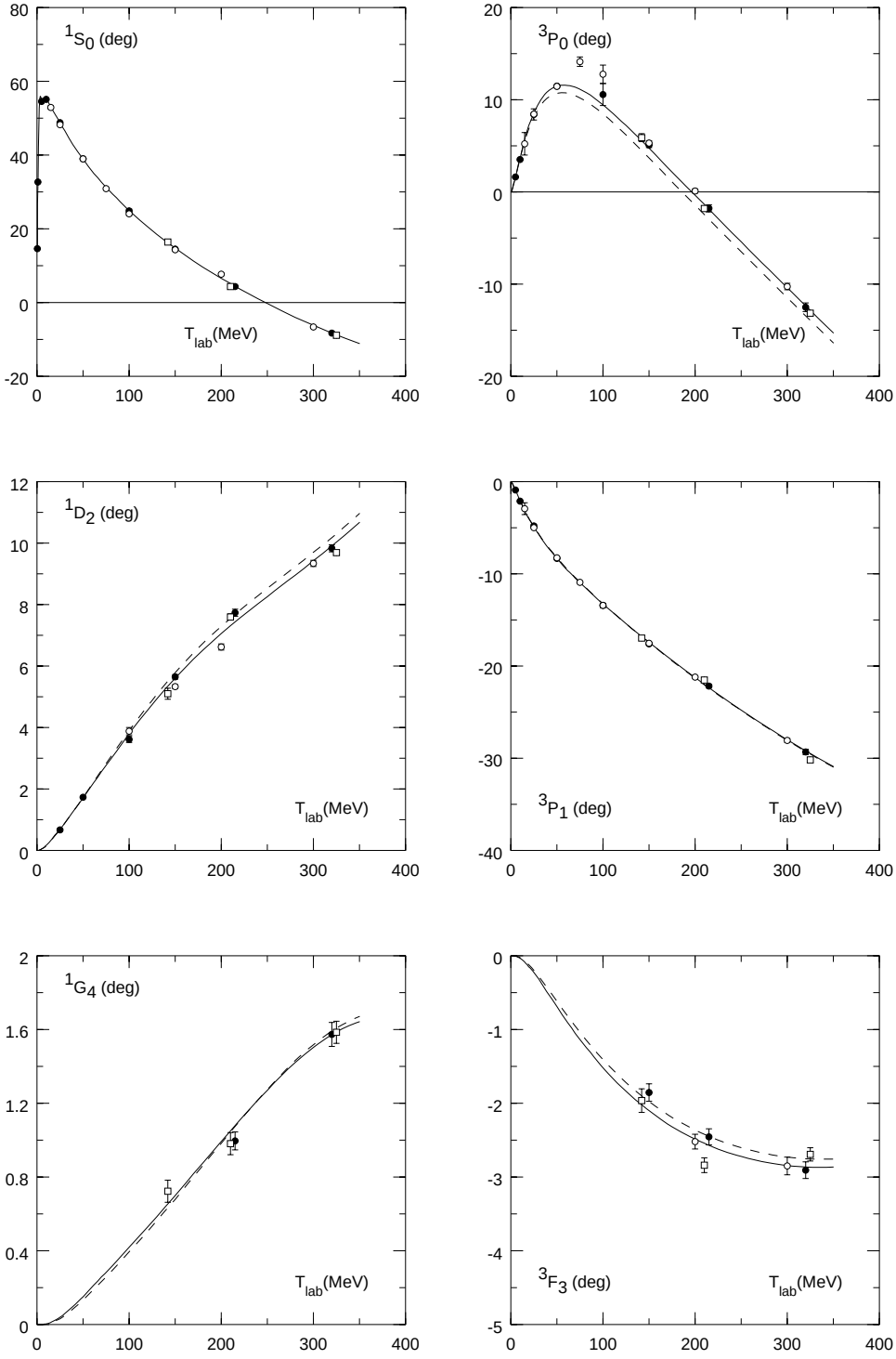

FIG. 4. Isovector phase shifts of the *pp* and *np* analyses in degrees vs $T_{\rm lab}$ in MeV. Solid line: multienergy *pp* values; dashed line: multienergy *np* values. •: single-energy *pp* values; ○: Arndt *et al.* [36]; □: Bugg [23].

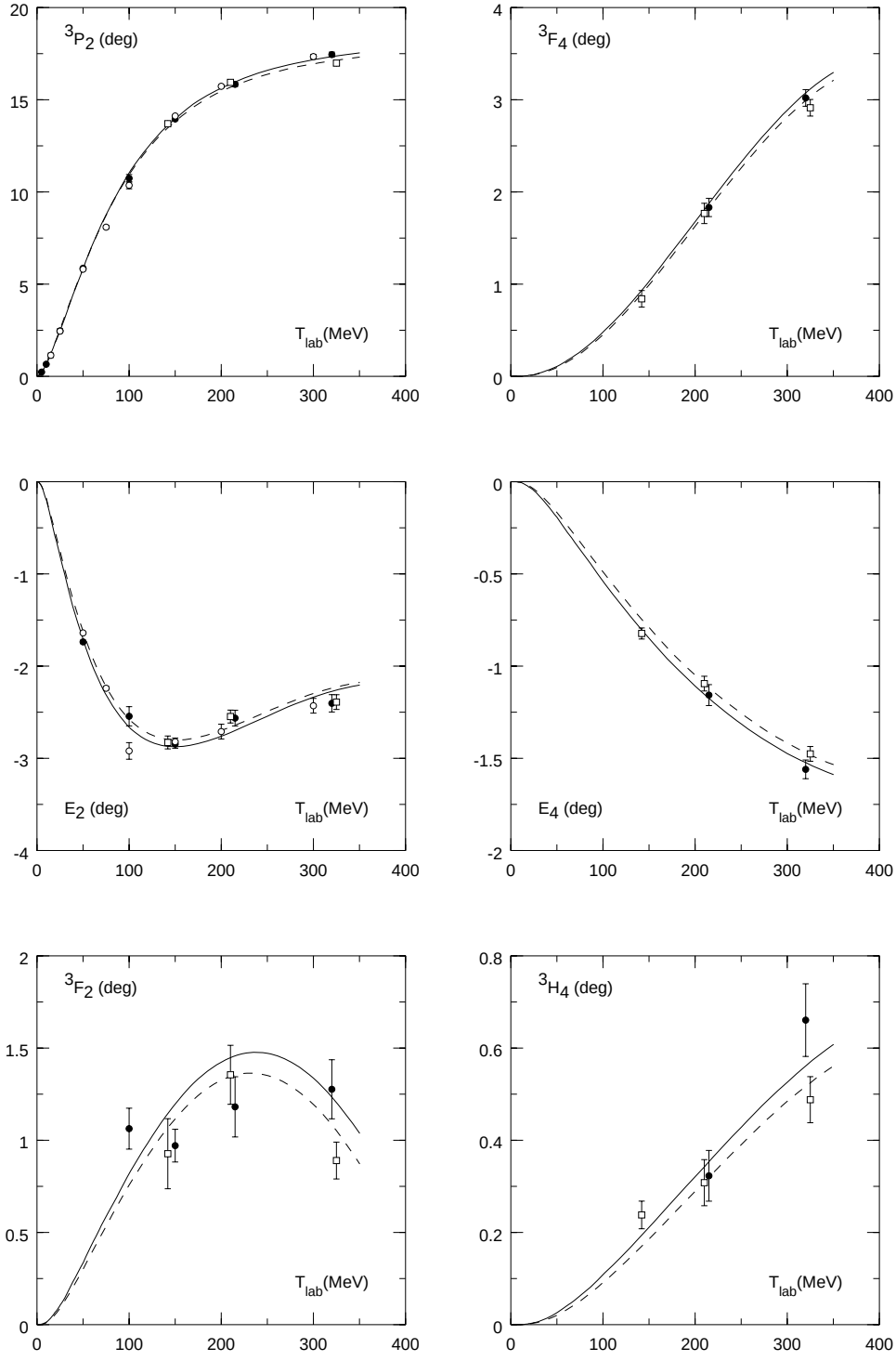

FIG. 4. continued

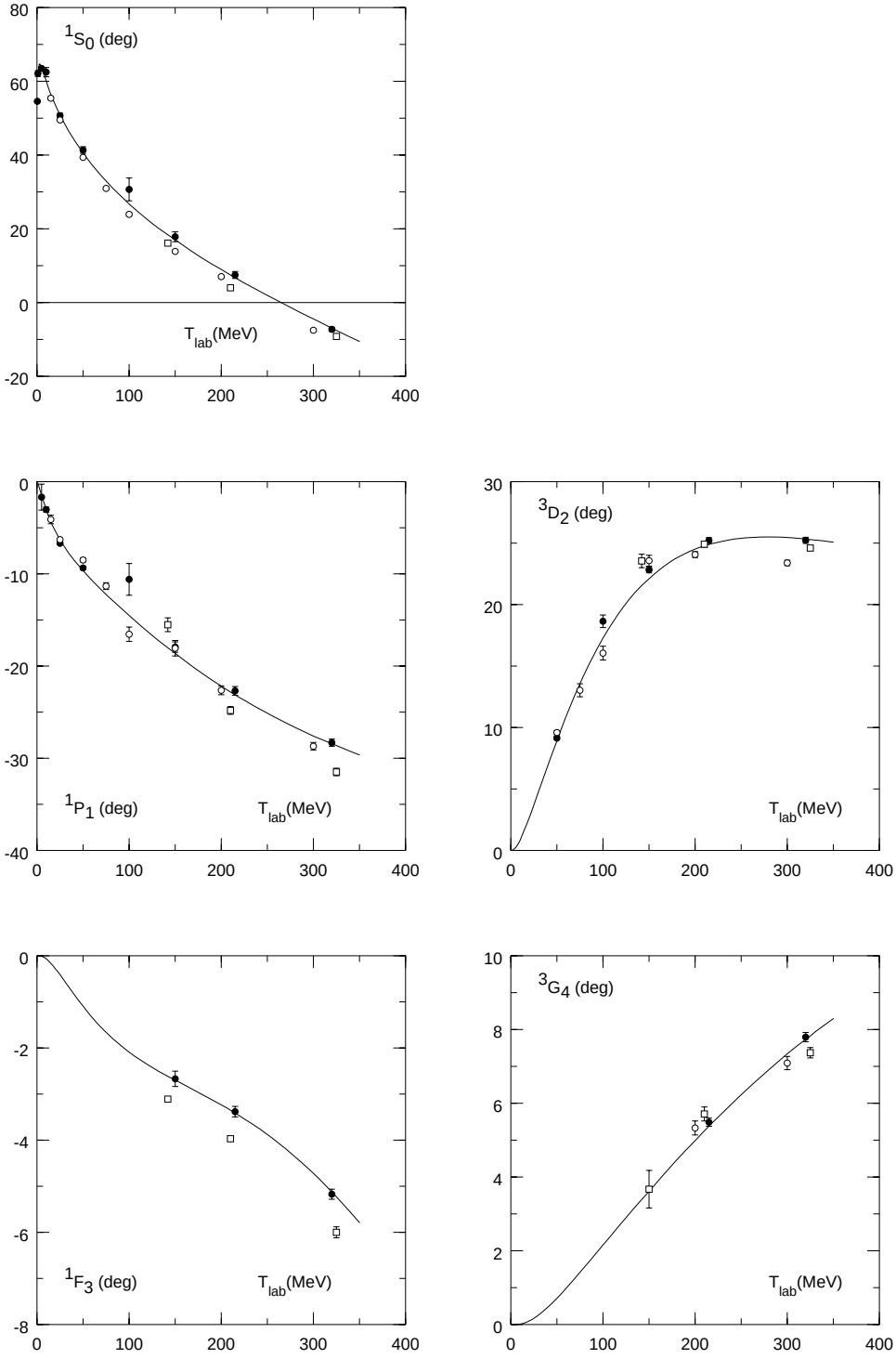

FIG. 5. Isoscalar phase shifts and $^1S_0$ phase shift of the *np* analysis in degrees vs $T_{\rm lab}$ in MeV. Solid line: multienergy *np* values. •: single-energy *np* values; ○: Arndt *et al.* [36]; □: Bugg [23].

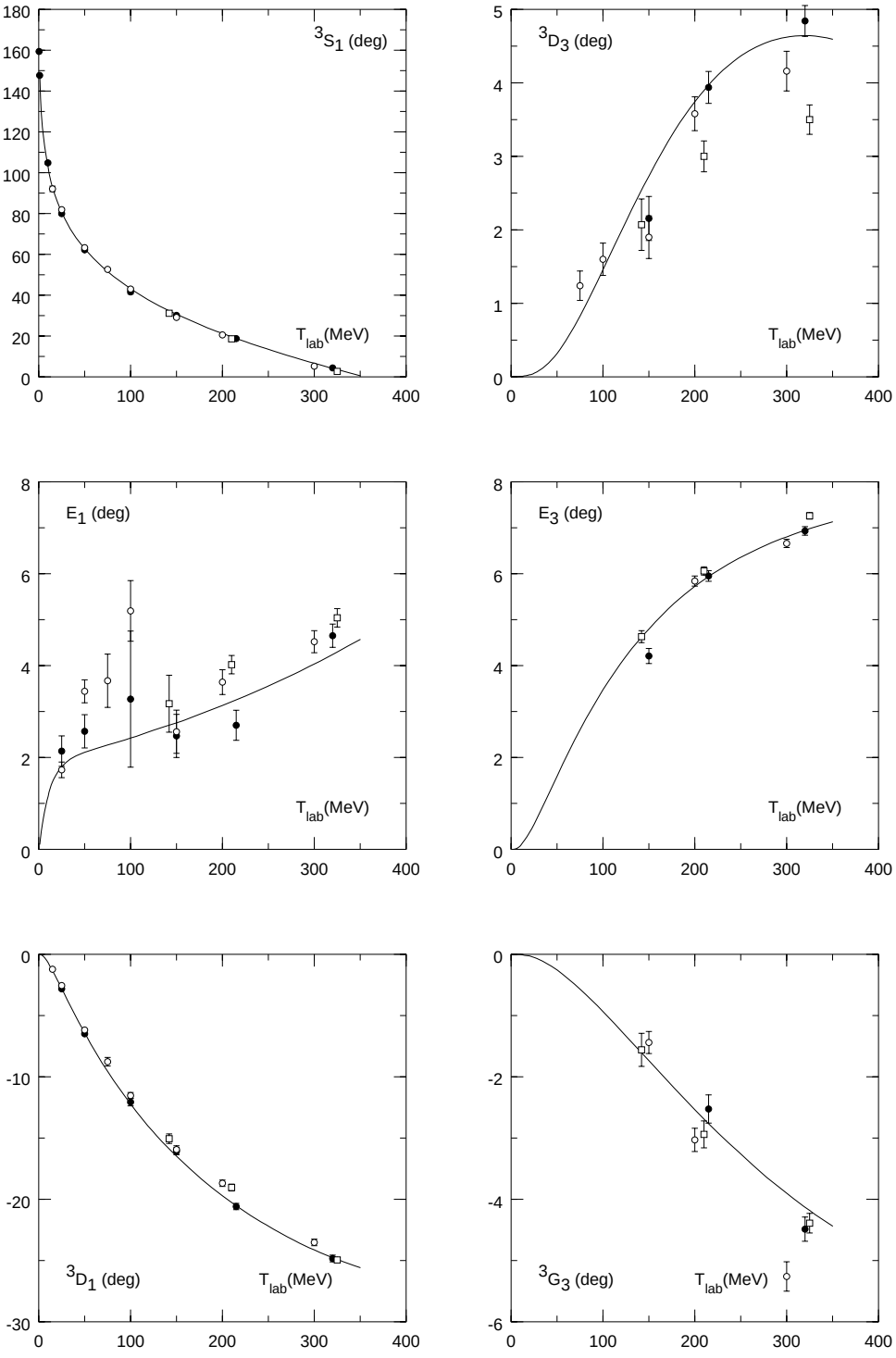

FIG. 5. continued